ON MODELS OF BONDING AND STRUCTURAL STABILITY IN HYDROCARBONS

by

WILLIAM CHADWICK MCKEE

(Under the Direction of Paul von Ragué Schleyer)

ABSTRACT

Aromatic rings, and aliphatic rings and chains comprise the backbone of organic chemistry. But while advances in quantum computational chemistry have facilitated accurate estimates of the observable properties of simple hydrocarbon species, qualitative and semi-quantitative models for understanding the predictions of theory are incomplete. The celebrated theoretical chemist Charles Coulson, after attending a scientific lecture, is rumored to have once remarked "give us insight, not numbers!" We strive here to heed Coulson's advice, and provide insight into the relative stabilities and bonding capacities of simple hydrocarbon systems of fundamental importance to organic chemistry. Branched alkanes have long been known to be more stable than their linear n-alkane isomers. This "alkane branching effect" is due to electron correlation effects arising from the greater number of 1,3 alkyl-alkyl interactions, called "protobranches," present in branched alkanes. Such protobranching interactions exist also in most linear and cyclic alkanes (e.g., the 1,3 methyl-methyl interaction in propane), and stabilize these species accordingly. In 1964 Heilbronner predicted that 4n π-electron annulenes might achieve closed shell stability, with no consequent loss in resonance energy, by adopting "Möbius-type" conformations which enforce a 180^{o} twist in their carbon p atomic orbitals. However despite being potentially stabilized by "Möbius aromaticity", neutral medium sized Möbius annulenes

are less stable than their untwisted Hückel counterparts. This is due in part to uneven p orbital twisting in Möbius isomers, which significantly reduces their resonance energies. Despite being Hückel aromatic, the 2π-electron cyclobutadiene dication and related isoelectronic derivative are all non-planar. Their puckering is caused by stabilizing cross-ring σ→π* hyperconjugation, which is possible only in non-planar geometries. Elementary Lewis bonding theory holds that carbon forms four 2-center 2-electron bonds. However the actual bonding capacity of carbon is not so confined, and neutral molecules exhibiting hexa and octavalent carbon atoms bound only to other carbons are possible. The hypervalent C-C interactions in these species are the result of electron deficient bonding, which ensures that the hypervalent carbon atoms obey the octet rule. The concepts developed in this thesis are general, and are expected to be transferable to a host of hydrocarbon species not considered herein.

INDEX WORDS: computational chemistry, protobranching, alkane branching effect, electron delocalization, hyperconjugation, resonance energy, aromaticity, Möbius aromaticity, Hückel Theory, natural bond orbitals (NBO), hypercoordinate carbon, hypervalent carbon, Quantum Theory of Atoms in Molecules (QTAIM), Energy Decomposition Analysis (EDA)

ON MODELS OF BONDING AND STRUCTURAL STABILITY IN HYDROCRABONS

by

WILLIAM CHADWICK MCKEE

B.S., University of Georgia, 2006

A Dissertation Submitted to the Graduate Faculty of The University of Georgia in Partial Fulfillment of the Requirements for the Degree

DOCTOR OF PHILOSOPHY

ATHENS, GEORGIA

2013

ON MODELS OF BONDING AND STRUCTURAL STABILITY IN HYDROCRABONS

by

WILLIAM CHADWICK MCKEE

Major Professor:	Paul von Ragué Schleyer
Committee:	Henry F. Schaefer III Robert J. Woods

Electronic Version Approved:

Maureen Grasso
Dean of the Graduate School
The University of Georgia
December 2013

DEDICATION

To my grandfather Bill Hollin.

ACKNOWLEDGEMENTS

I wish to express my sincere gratitude to the following people whose contribution to my scientific development is difficult to overstate. Thanks to Keigo Ito for mentorship in the early days of my graduate studies, and friendship later on. Thanks to Judy Wu for many interesting personal and scientific discussions, and a valuable friendship. Thanks to Prof. Henry Schaefer for fostering an outstanding environment in which to study computational chemistry. Attending your weekly group meetings inspired me to learn many mathematical aspects of chemistry I otherwise would likely not have. Finally, thank you Prof. Paul Schleyer for teaching me how to "be" a scientist, how to write (or at least showing me what good scientific writing looks like!), and for all of the intriguing projects and collaborations that come with working under the direction of a celebrated chemist.

TABLE OF CONTENTS

Page

LIST OF TABLES

Page

LIST OF FIGURES

Page

CHAPTER 1

INTRODUCTION

During a casual conversation, my Ph.D. advisor, Paul Schleyer, once commented that "hydrocarbons units comprise the backbone of organic chemistry." The truth of this statement is self-evident to any organic chemist, as is the fundamental importance of understanding the relative energetic stabilities of simple hydrocarbon conformational and configurational isomers. However, one might regard scientific "understanding" as being comprised of two parts, namely its quantitative and qualitative aspects. For example, to understand the relative stability of n-pentane vs. isopentane, we must first quantitatively determine the relative energies of these species. This can be done, e.g., computationally, by performing *ab initio* self-consistent field (SCF) computations to estimate the total energies of n-pentane and isopentane. We might then refine our results to include electron correlation effects. Other improvements are also possible. Given an appropriate theoretical approach, our final quantitative estimate will reveal that isopentane is more stable than n-pentane by about 1.65 kcal/mol, the experimental value at 0 K. But this is only half of the picture. We can hardly claim to understand our result unless we can explain why it occurs. Moreover, without qualitative comprehension, we are left with no indication of whether the third pentane isomer, neopentane, is more stable than isopentane, less stable than n-pentane, or somewhere in between. What is the stability ordering of the various isomers of hexane? What of the next simple case we might imagine? Are computations and experiments our only recourse?

Such questions highlight the need for qualitative and semi-quantitative models for interpreting and explaining chemistry. Often however, the underlying causes of a physically observable property are not themselves observable. Hence these models frequently employ virtual (i.e., non-measurable) properties to explain chemical behavior. Examples of such properties include bonds, resonance, aromaticity, steric repulsion, hyperconjugation, electron correlation, etc. As none of these are directly measurable, theory is the natural avenue for their characterization and quantification. However, the non-measurability of such virtual properties has led to various models which compete to define them. As of the time of this writing, the issue of which model(s) "best" describe chemical behavior is far from settled.

For example "steric repulsion" is commonly associated with the Pauli Exclusion Principle, which prevents same spin electrons from occupying the same region of space. Hence, we might relate steric repulsion to the energetic penalty of requiring that molecular orbitals (or localized molecular orbitals) be orthogonal to one another. This is the approach adopted by Natural Bond Orbital (NBO) Steric Analysis, as well as several energy decomposition analysis (EDA) schemes. However, the choice of the "best" non-orthogonal orbital set differs in the NBO and EDA formalisms, leading to disparate numerical estimates of steric repulsion.

π-Resonance stabilization is due to the energy lowering effects associated with π-electron delocalization over multiple atomic centers. Hence, resonance energies may be quantified by comparing the stability of a molecule with a delocalized π-system to a species with localized π bonds. Notably the choice of an appropriate "localized" reference standard is not unique. Hückel Molecular Orbital (HMO) Theory derives π-resonance energies by comparing the HMO total π-electron energy of a conjugated hydrocarbon to that of ethylene. Alternatively NBO

analysis evaluates π-resonance effects by comparing the energy of molecule to that of the same molecule described by a (hypothetical) wavefunction where π-electron delocalization is disallowed. Other theoretical evaluations of resonance energies also are commonly employed.

As a final example we might consider the most famous and useful of all virtual properties: the chemical bond. No universally accepted quantum mechanical definition of bonding exists, but bonds are generally associated with electron sharing and short interatomic distances between atoms, as well as significant energy lowering associated with bond formation. Again the quantitative aspects of theory are useful tools for developing a concept of bonding. Electron sharing between atoms may be evaluated by the degree of electron density accumulation between atomic centers, which is the approach adopted by the Quantum Theory of Atoms in Molecules (QTAIM), as well as many localized molecular orbital (LMO) schemes. Distances between bound atoms are obviously determined from the geometries of computed stationary point structures. Finally, the energy lowering associated with bond formation can be assessed by the energy change of appropriately defined chemical equations which isolate the effects of bonding. Importantly the choice of how to define an interatomic distance is not ambiguous, but comparable definitions of "electron density accumulation" and "appropriately defined equations" for assessing bond strengths are left to our better judgment.

There is thus considerable room for flexibility and exploration of the meaning of the various virtual quantities that guide our models for understanding chemistry. We anticipate that the best models and concepts will be those which are most transferable to a wide variety of systems, and best able to predict the properties of as yet unknown systems. This dissertation critically examines and further develops models of structural stability and bonding in

hydrocarbons. We employ both quantitative (i.e., observable) and qualitative (virtual) concepts to guide our understanding. Chapter 2 examines the "alkane branching effect," which denotes the fact that simple branched alkanes (e.g., neopentane) are more stable energetically than their less branched isomers (e.g., isopentane and n-pentane). Two models, one based on intramolecular attractive interactions, and the other based on repulsive interactions compete to explain this effect. Careful analysis of the correlation energies of alkane isomers reveals the former model is decidedly more consistent with the available theoretical data.

Chapter 3 concerns the resonance energies of Möbius and Hückel [n]annulenes. An older Hückel Molecular Orbital Theory model of their π-delocalization energies, based on assumed planar geometries, is shown to be inadequate. Hence an adaptation of Hückel Theory is proposed which accounts for the uneven twisting of carbon p atomic orbitals (AO) resulting from the non-planarity of medium sized [n]annulene systems. This theory is shown to partially account for why neutral Möbius [n]annulenes have yet to be observed experimentally.

Chapter 4 explores the factors responsible for the surprising non-planarity of Hückel aromatic 2π-electron 4-membered rings. Two alternative effects, namely cross ring partial 1,3 bonding due to p AO overlap, and cross ring $\sigma \rightarrow \pi^*$ hyperconjugation in non-planar rings are considered as possible origins. Optimization of 2π-electron 4-membered rings in the absence of cross ring $\sigma \rightarrow \pi^*$ hyperconjugation leads to ring planarity in all cases considered, supporting the latter explanation.

Finally Chapter 5 challenges a core tenant of elementary Lewis bonding theory: the tetravalency of carbon. Examples of compounds containing hexa and octavalent carbon atoms are presented. The hypervalent carbons in these species are coordinated to only other carbon

atoms, and many of the proposed compounds are neutral. A new bonding theory for these carbon atoms, based on 2-center electron deficient bonds (EDB), is proposed to rationalize the C-C interactions in these compounds. This EDB mechanism violates the Lewis electron pairing rule, but preserves the octet rule. We hope that both this and the other theories of hydrocarbon bonding and structural stability presented herein will enrich chemist's understanding of the carbon "backbones" of organic and biochemistry.

CHAPTER 2

CORRELATION EFFECTS ON THE RELATIVE STABILITIES OF ALKANES

-W. C. McKee, P. v. R. Schleyer, 2013, J. Am. Chem. Soc., 135, 13008-13014, Reprinted here with permission of publisher.

2.1 ABSTRACT

The “alkane branching effect” denotes the fact that simple alkanes with more highly branched carbon skeletons, for example, isobutane and neopentane, are more stable than their normal isomers, for example, n-butane and n-pentane. Although n-alkanes have no branches, the “kinks” (or “protobranches”) in their chains (defined as the composite of 1,3 alkyl-alkyl interactions−including methine, methylene, and methyl groups as alkyl entities−present in most linear, cyclic, and branched alkanes, but not methane or ethane) also are associated with lower energies. Branching and protobranching stabilization energies are evaluated by isodesmic comparisons of protobranched alkanes with ethane. Accurate *ab initio* characterization of branching and protobranching stability requires post-self-consistent field treatments, which account for electron correlation. Localized molecular orbital second-order Møller−Plesset (LMO-MP2) partitioning of the correlation energies of simple alkanes into localized contributions indicates that correlation effects between electrons in 1,3-alkyl groups are largely responsible for the enhanced correlation energies and general stabilities of branched and protobranched alkanes.

2.2 INTRODUCTION

Nearly 80 years have passed since it was established that branched alkanes like isobutane and neopentane are more stable energetically than their "normal" isomers, n-butane and n-pentane.[1,2] Since then myriad proposed explanations of this "branching effect" have appeared,[3−23] but general consensus regarding the origins of branching stability is still lacking. One of the first and best known explanations is that of Pitzer and Catalano,[8] who suggested that the electron correlation energies of more highly branched alkane isomers exceed those of their less branched counterparts. Though they never speculated which intramolecular interactions were responsible for the greater correlation energies of branched alkanes, modern *ab initio* studies have now definitively established that reliable branching energies are reproduced only by electron correlated methods and that Hartree−Fock and density functional theory (DFT) treatments which do not adequately account for such correlation effects fail to recover the alkane branching effect satisfactorily.[17a,21,25−38]

Another explanation for branching stability supposes that imbalances in geminal electron delocalization (i.e., resonance or hyperconjugation between adjacent bonds) effects favor branching in isomeric alkanes. Interest in hyperconjugative models of alkane branching first appeared in the early work of Brown,[6] Dewar et al.,[7] and Pople and Santry[10] and has been recently renewed. Inagaki[14] argued that electron delocalization from C−H to vicinal C−C bonds favors branching in alkanes, and Kemnitz et al.[22] suggested that increased C−C−C geminal hyperconjugation is responsible for the branching effect. Such studies provide insight into the origins of branching stability at the self-consistent field (SCF) level, but the question of why electron correlation effects strongly stabilize branched alkanes remains unsettled.

Based on the early ideas of Bartell et al.,[11,24] Gronert[18] advanced a geminal repulsion model of alkane branching, positing that more highly branched alkanes are subject to decreased intramolecular repulsion compared to their less branched isomers. However, Bartell39 has recently criticized Gronert's model, and several theoretical studies indicate that alkane branching increases intramolecular repulsions. Laidig[13a] showed that the repulsive (energy raising) components of the Hartree−Fock Hamiltonian, that is, electron−electron repulsion, nuclear−nuclear repulsion, and the electron kinetic energy, all increase with increasing branching in alkanes but are overcome by an even larger increase in electron nuclear attraction.[13b] De Proft et al.'s[21] DFT energetic component analysis also suggests that branched alkanes are destabilized by increased Pauli exchange and classical electrostatic repulsions but that greater electrostatic attraction and electron correlation stabilization overcome these effects, giving rise to branching stability. Finally, Kemnitz et al.'s[22] natural bond orbital steric analysis[40] of geminal Pauli-exchange repulsions in alkanes also found that branching in alkanes increases their intramolecular repulsion. Each of these works indicates that branching stability is an attractive dominant process (i.e., governed by attractive interactions).

Our "protobranching" model, based on the effect of electron correlation,[17a] attributes the enhanced stability of branched alkanes to their greater number of 1,3-alkyl−alkyl interactions, or "protobranches" (taking methine, methylene, and methyl groups of alkanes as alkyl units, cf. Figure 1). The simplest example of a protobranching interaction is the 1,3-methyl−methyl interaction in propane. However, 1,3 methyl−methylene and methylene−methylene interactions also constitute protobranches, and their near-energetic equivalence to 1,3-methyl−methyl interactions is suggested by the nearly constant (ca. 5 kcal/mol) increase in n-alkane heats of

formation along the series propane, n-butane, n-pentane, and so forth. As originally conceived, "protobranching" is a descriptive term designating "the onset of branching." The designation "protobranch" was introduced to call attention to the structural relationship between the "kinked" geometry of propane (and other n-alkanes) and the similar "kinks" in branched alkanes, like isobutane and neopentane.

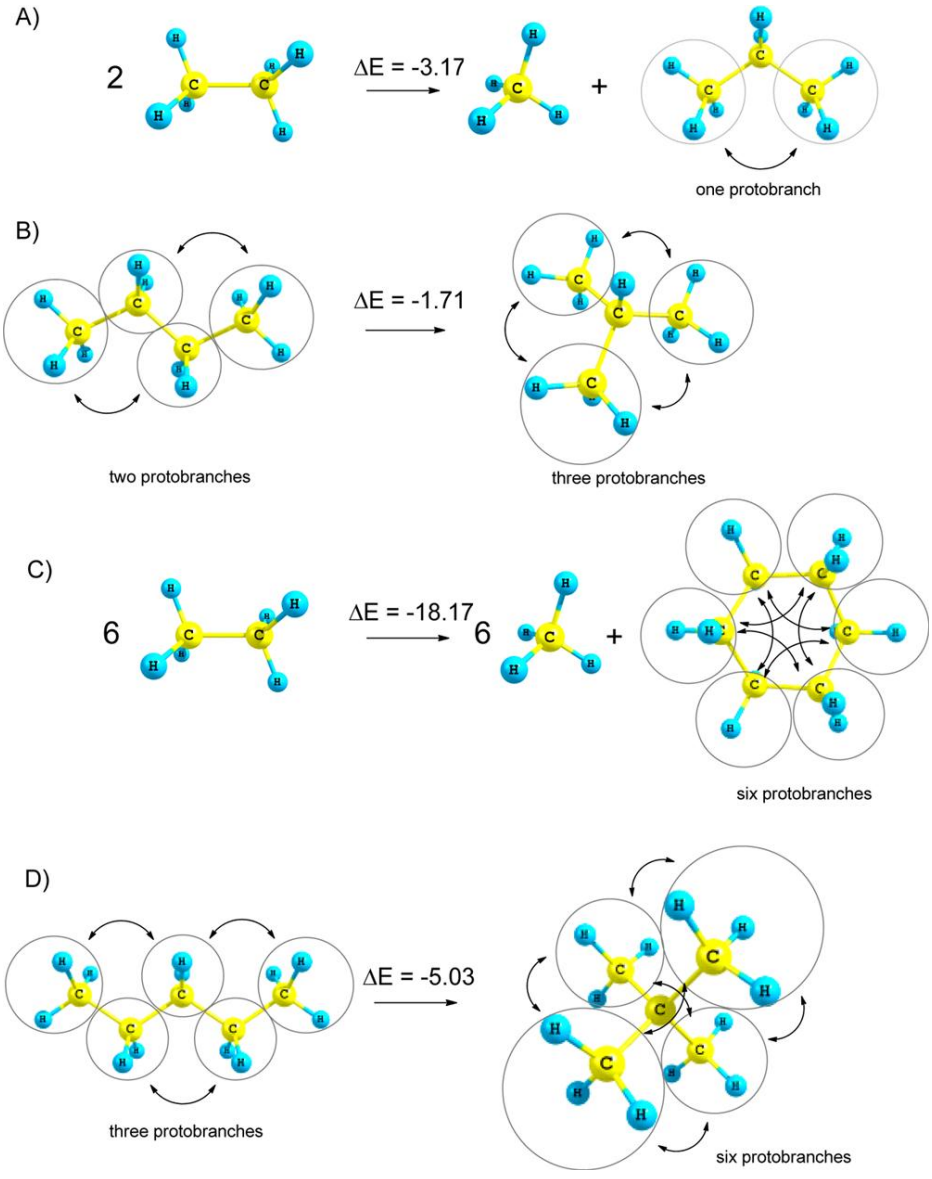

Figure 2-1. Equations for evaluating protobranching (A, C) and branching (B, D) stabilization. Energy changes (kcal/mol) are taken from experimental heats of formation data at 0 K.[42]

Propane is the smallest alkane with a protobranch, since by definition, by usage, and by analogy with isobutane and neopentane, there must be an open edge lacking a conventional bond.[17a] The energy-lowering effects of "protobranching" refer to the "net stabilizing composite of 1,3-alkyl−alkyl interactions not present in methane or ethane."[17b,41] Such protobranching stabilization involves all of the various nonbonded interactions among all the 1,3-alkyl−alkyl group atoms, for example, 1,4- and 1,5-interatomic interactions.

Our previous discussion of the protobranching concept[17] focused on the interpretive implications of regarding 1,3-alkyl−alkyl interactions as stabilizing, postponing detailed exploration the underlying origins of this "attraction" (i.e., stabilization). We examine here the origins of the strong electron correlation stabilization of branched and protobranched alkanes and the extent to which 1,3-alkyl−alkyl interactions are responsible. We note that electron correlation effects are not the only source of branching and protobranching stability. In some cases, SCF treatments recover a portion of this stabilization, and the ZPVEs of alkane isomers also favor branching. However, these contributions to the branching effect have been examined in detail elsewhere.[6,7,10,12,13,21,22,34]

2.3 RESULTS AND DISSCUSSION

Redfern et al.[25] noted more than 10 years ago that theoretical treatments which do not properly account for electron correlation effects fail to describe alkane isomerization energies adequately;

since then these shortcomings have been welldocumented.[26−37] Similarly, such treatments also fail to recover protobranching stabilization satisfactorily, for example, the enhanced stability of linear alkanes with 1,3-alkyl−alkyl interactions relative to ethane. This problem has been evaluated extensively by assessing the errors associated with theoretical evaluations of the energy change of eq 1, where the product alkane is taken to be the linear isomer.[28,33,36,38]

$$(m-1)C_2H_6 \rightarrow C_mH_{2m+2} + (m-2)CH_4 \qquad (1)$$

Moreover, even greater errors are encountered when the product of eq 1 is taken to be the most branched isomer (which contains more protobranching interactions). For illustrative purposes Table 1 presents these errors at the HF, B3LYP, B3LYP-D3, and MP2 levels (far more extensive tabulations may be found elsewhere).[28,33,36,38] The comparisons between theory and experiment presented in Table 1 are subject to the usual caveats regarding the limitations of the harmonic frequency approximation,[43] but clearly protobranching stabilization is not adequately described at the HF or B3LYP levels. Appending the empirical "D3" dispersion correction44 to the B3LYP functional improves agreement between theory and experiment, but significant discrepancies remain,[45] and similar errors have also been reported for the popular M06 family of functionals.[36,38] Only the MP2 values in Table 1 match experimental data, underscoring the need for post-SCF treatments when computing of the energy change of isodesmic or isomerization equations which are protobranching imbalanced. Of course, more accurate protobranching energies may be obtained by employing higher levels of theory (see refs 33, 43, and 46 for high-

accuracy computations of alkane energies), but we are concerned here with understanding why electron correlation effects preferentially stabilize branched and protobranched alkanes.

equation	HF	B3LYP	B3LYP-D3	MP2	expt
2 ethane → propane + methane	−1.66 (+1.51)	−1.92 (+1.25)	−2.44 (+0.73)	−3.14 (+0.03)	−3.17
3 ethane → butane + 2 methane	−3.37 (+3.38)	−3.89 (+2.86)	−5.03 (+1.72)	−6.47 (+0.28)	−6.75
3 ethane → isobutane + 2 methane	−3.97 (+4.49)	−4.67 (+3.79)	−6.29 (+2.17)	−8.59 (−0.13)	−8.46
4 ethane → pentane + 3 methane	−5.06 (+5.10)	−5.81 (+4.35)	−7.61 (+2.55)	−9.81 (+0.35)	−10.16
4 ethane → neopentane + 3 methane	−6.04 (+9.15)	−7.21 (+7.98)	−10.51 (+4.68)	−15.50 (−0.31)	−15.19
5 ethane → hexane + 4 methane	−6.78 (+6.81)	−7.78 (+5.81)	−10.24 (+3.35)	−13.18 (+0.41)	−13.59
5 ethane → 2,2-dimethylbutane + 4 methane	−5.04 (+11.74)	−7.04 (+9.74)	−11.64 (+5.14)	−17.80 (−1.02)	−16.78
6 ethane → heptane + 5 methane	−8.50 (+8.52)	−9.73 (+7.29)	−12.85 (+4.17)	−16.56 (+0.46)	−17.02
6 ethane → 2,2,3-trimethylbutane + 5 methane	−3.14 (+16.47)	−6.31 (+13.30)	−12.84 (+6.77)	−21.20 (−1.59)	−19.61
7 ethane → octane + 6 methane	−10.22 (+10.23)	−11.71 (+8.74)	−15.49 (+4.96)	−19.95 (+0.50)	−20.45
7 ethane → 2,2,3,3-tetramethylbutane + 6 methane	+0.02 (+23.15)	−4.50 (+18.63)	−13.56 (+9.57)	−25.57 (−2.43)	−23.13

[a]Errors relative to experiment are given in parentheses. Computational data include ZPE corrections.

Table 2-1. Energy changes of selected isodesmic equations involving alkanes given by experimental heats of formation data at 0 K.[42a] and the HF, B3LYP, B3LYP-D3, and MP2 levels (cc-pVTZ basis set).[a]

Clearly, branched alkanes are stabilized by electron correlation effects relative to their less branched isomers because their structures and hence electron distributions are more compact. This is demonstrated by the decrease in the molecular surface areas of simple alkane isomers with increasing branching. Similarly, the products of eq 1, which evaluates protobranching stabilization, also have a lower combined surface area than the reactants (Figure 2). Moreover, a linear relationship exists between the decrease in the total molecular surface area of the products of eq 1 relative to the reactants and their enhanced stability due to electron correlation effects (Figure 2 plots this data for all possible alkane products of eq 1 where $3 \leq m \leq$

7). This trend illustrates a general relationship among alkanes with 3−7 carbon atoms between the number protobranching interactions they contain, their molecular compactness, and their correlation energy.

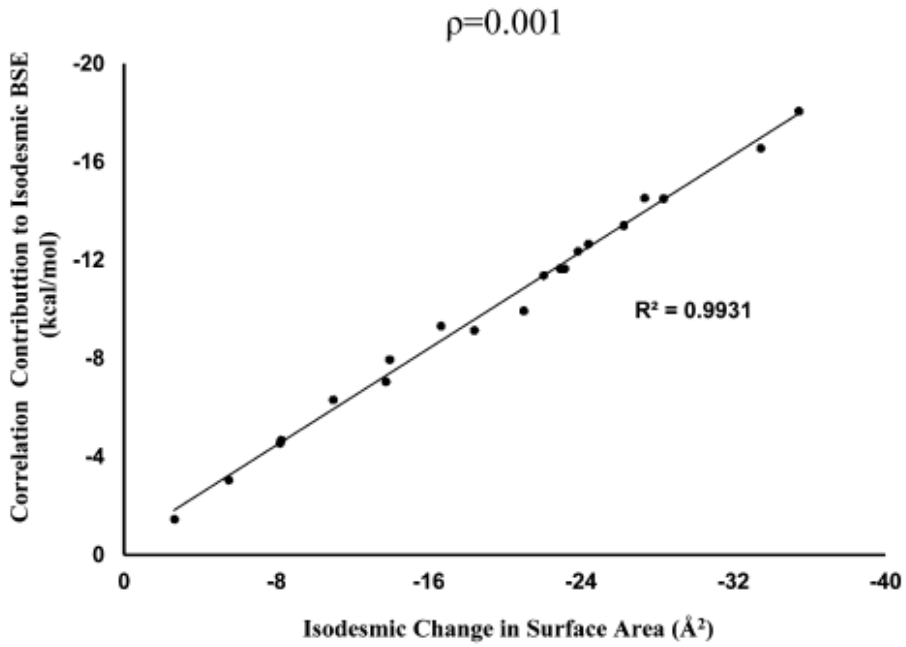

Figure 2-2. Correlation contribution ($\Delta E_{[MP2]} - \Delta E_{[HF]}$, kcal/mol) to the change in electronic isodesmic bond separation energy (BSE) of eq 1 for all alkane products with 3−7 carbon atoms vs the change in molecular surface area (Å^2). Results are based on MP2/cc-pVTZ geometries. Molecular surface areas were computed in Chimera[47] with $\rho = 0.001$.

But can the correlation stabilization of branched and protobranched alkanes be explained in terms of specific intramolecular interactions? To examine this we partition the MP2 correlation energy into localized contributions as in Grimme's[26] 2006 survey of branching

stabilization.[48] The frozen-core MP2 correction ($E^{(2)}$) to the HF energy may be interpreted physically as the sum of individual two-electron correlation energies between all possible pairs of valence electrons in a molecule. These electron-pair correlation energies, or "pair energies" more simply, are usually evaluated between two electrons in canonical MOs and hence are not easily interpretable in terms of specific intramolecular interactions. However, since the MP2 correction is invariant to unitary transformations of the occupied MOs, the same correlation energy is obtained whether canonical or localized MOs (LMO) are used as a basis for an MP2 treatment.[49a] The advantage of LMO-MP2 is that the total correlation energy of a molecule can be partitioned into additive contributions from electron pairs occupying localized bonding or lone pair orbitals. Each localized pair energy is typically classified as being either an "intrapair" energy, which results from correlation effects between two electrons occupying the same LMO, or an "interpair" energy, which corresponds to correlation effects between two electrons each in different LMOs. We emphasize that the designation "LMO-MP2" refers to an MP2 treatment with localized occupied orbitals and canonical virtual orbitals, which differs from local correlation methods (e.g., LMP2) which localize both occupied and virtual orbitals as a means of improving the computational efficiency of post-SCF levels of theory.[49b]

Grimme's[26] LMO-MP2 decomposition of the branching effect revealed that the intrapair correlation energies of isomeric alkanes are essentially equal, and hence that branching stabilization results solely from interpair correlation effects (i.e., correlation between pairs of electrons in different orbitals). The result is sensible as isomers necessarily contain the same number and types of bonds but differ in intramolecular interactions. Grimme also partitioned electron interpairs into groups based on the distance between the centroids of the two LMOs

occupied by each electron of a given pair and showed that the bulk of branching stability results from electron correlation effects over medium range distances (i.e., ~1.5−3.0 Å). An alternative partitioning of interpair energies is advantageous for our purposes. We divide interpairs into groups based on the spatial relationship of the LMOs each electron of a given pair occupies. Two electrons occupying LMOs in a geminal relationship are denoted a 1,2-pair; those occupying vicinal LMOs are a 1,3-pair, and so forth. Examples of this partitioning scheme, which essentially divides the electron correlation energies of alkanes into geminal (1,2), vicinal (1,3), and longer range correlation contributions (1,N where N ≥ 4) are depicted in Figure 3.

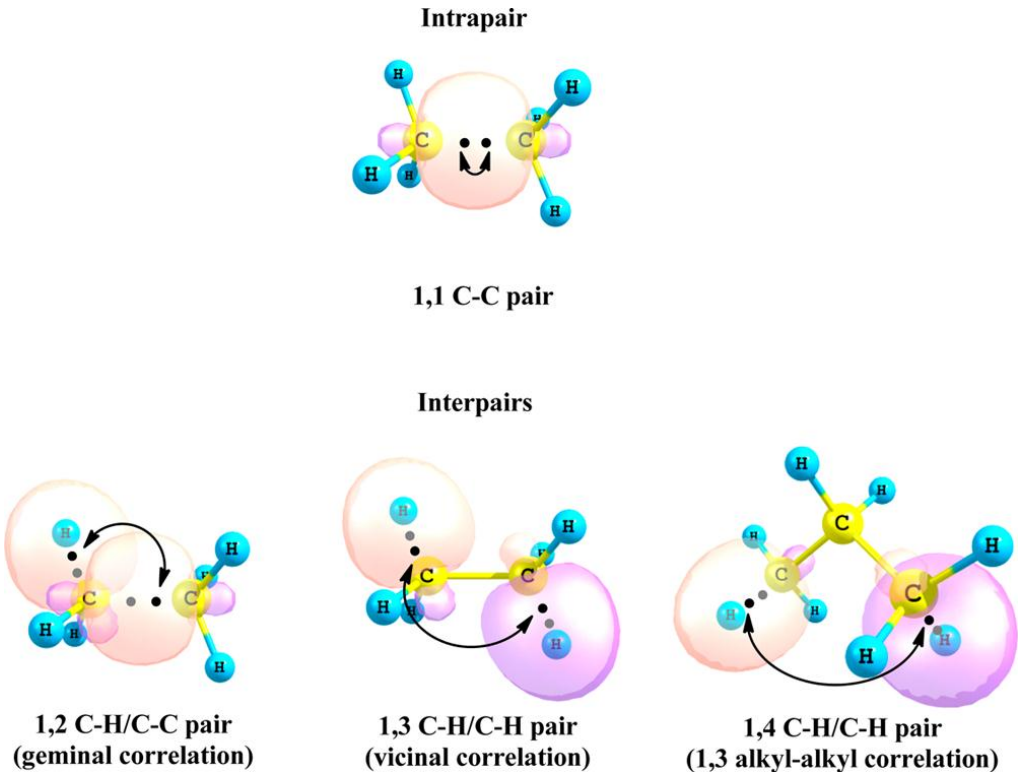

Figure 2-3. Representative examples of the pair energy partitioning used in this work. An "electron pair" consists of two electrons in either the same LMO (intrapair) or two electrons in separate LMOs (interpair).

Note that in an LMO basis, 1,3-alkyl−alkyl interactions correspond precisely to 1,4-electron pairs, since 1,3-pairs are present in ethane, which experiences vicinal correlation effects but contains no protobranches, while 1,5 and more distant pairs are not present in propane, the smallest protobranched alkane.

Table 2 presents the changes in intrapair and 1,N interpair correlation energies for several isodesmic and isomerization equations involving simple alkanes. We employed Pipek−Mezey orbital localization,50a but alternative localization methods (e.g., the Boys,[50b] minimum population,[50c] and Ruedenberg[50d] methods) give similar results. If 1,3-alkyl−alkyl interactions are responsible for branching and protobranching stability, then 1,4-pair energies are expected to contribute dominantly to the electron correlation stabilization of protobranched and branched alkanes, respectively. This is clearly the case for the protobranching stabilization of propane (eq a in Table 2). The changes in intrapair and vicinal (i.e., 1,3) interpair correlation energies are small and stabilize the reactants, while the change in the 1,2-interpair correlation is nearly zero. Thus 98% of the interpair correlation stabilization of the products is due to 1,4-pair correlation effects between the C−H bonds in the methyl groups of propane (see Figure 3 for a representative example), which have no counterpart in ethane or methane. The changes in pair energies of eqs b and c in Table 2, which evaluate the branching stabilization of isobutane and neopentane, are largely similar. Aside from a relatively small stabilization from geminal

correlation effects, the bulk of the enhanced electron correlation stabilization of isobutane and neopentane relative to n-butane and n-pentane is due to increased 1,4-interpair stabilization. This corresponds again to correlation effects between pairs of C−H bonds in 1,3-methyl groups.

The trends in Table 2 result largely from imbalances in the number of 1,N interpairs between the reactants and products and the fact that the magnitude of interpair energies decreases sharply (approximately as 1/r6)49 as the distance between the two LMOs occupied by an given electron pair is increased. For example, although 1,2- and 1,3-pair interactions are largest in magnitude, their numbers are balanced in eqs a−d. Thus there are only small discrepancies in their sums between the reactants and products, which are due mainly to differences in the types of geminal and vicinal bonds being correlated (e.g., eqs a and b trade two 1,3-C−H/C−C interpairs for one 1,3-C−C/C−C and one 1,3-C−H/C−H interpair). In contrast, the number of 1,4-pair energies in eqs a−c is not balanced. Indeed any isodesmic or isomerization equation involving only alkanes which is not protobranching balanced cannot balance the number of 1,4-interpairs, as 1,3-alkyl−alkyl correlation effects and 1,4-pair energies are equivalent in such cases. Hence, the 1,4-interpair stabilization of propane, isobutane, and neopentane arises simply because they contain more 1,4-interpairs than the reactants in eqs a, b, and c. Ethane has no protobranches and hence no 1,4-interpairs, while the isomerization of n-butane to isobutane and n-pentane to neopentane trades 1,5 (and in the case of n-pentane also 1,6) interpairs for 1,4-interpairs. Since 1,4-pair energies are larger than those of the 1,5- and 1,6-types, this trade is favorable. Indeed 1,5- and longer range correlation effects generally contribute little to the relative stabilities of simple alkanes. This is illustrated by eq d in Table 2, which is protobranching balanced, and as a result conserves the numbers of 1,2-, 1,3-, and 1,4-interpairs

between reactants and products. The MP2 correction to the HF energy change is small in this case, as the 1,5-pairs energies of butane, which correspond to long-range dispersion interactions, only weakly favor the products. Since no substantial correlation contribution to the reaction energy exists, it is not surprising that the HF and DFT treatments which do not accurately describe protobranching stabilization predict the energy change of eq d to within less than half a kilocalorie of the −0.41 kcal/mol experimental value at 0 K.[42,51] This further highlights that the failure of such methods to adequately reproduce protobranching energies results principally from deficiencies in their description of medium range electron correlation effects.

	$\Delta e^{(2)}_{intra}$	$\Delta e^{(2)}_{1,N\text{-inter}}$					
	1,1	1,2	1,3	1,4	1,5	1,6	$\Delta E^{(2)}$
(a) 2 ethane → propane + methane	+0.20	0.04	+0.17	−1.80			−1.47
(b) *n*-butane → isobutane	+0.11	−0.22	+0.43	−2.06	+0.24		−1.50
(c) *n*-pentane → neopentane	+0.24	−0.57	+1.43	−6.23	+0.46	+0.05	−4.62
(d) 2 propane → *n*-butane + ethane	+0.02	+0.08	−0.03	+0.05	−0.24		−0.12

[a]Electronic energies (in kcal/mol) were computed at the MP2/cc-pVTZ level.

Table 2-2. Change in the sum of intrapair and 1,N-Interpair correlation energies ($\Delta e^{(2)}_{intra}$ and $\Delta e^{(2)}_{1,N\text{-inter}}$) along with the total change in correlation energy ($\Delta E^{(2)}$) for selected equations.[a]

The stabilization of propane, isobutane, and neopentane by 1,3-alkyl−alkyl correlation effects also is present in other linear, branched, and cyclic alkanes. This is apparent from Table 3, which evaluates the correlation contribution to a variety of protobranching imbalanced isodesmic and isomerization equations. While the intrapair contribution to each reaction energy is small, the interpair correlation energy stabilizes the more highly protobranched products, predominately due to their greater number of 1,4-interpairs. The large protobranching energy of

cyclohexane (given by the eq: 6 ethane → cyclohexane + 6 methane) is particularly noteworthy. Though generally considered to be "strain free", cyclohexane, like neopentane, contains six protobranching interactions and exhibits comparable protobranching stabilization (−12.62 vs −11.93 kcal/mol, respectively, see Table 3). Hence, rather than being regarded as a strain free paradigm, cyclohexane has a considerable "negative strain".

	ΔE_{HF}	ΔE_{MP2}	$\Delta E^{(2)}$	$\Delta e^{(2)}_{intra}$	$\Delta e^{(2)}_{inter}$	% $\Delta e^{(2)}_{inter}$ stabilization due to 1,4-pair energy imbalances
Protobranching Equations						
2 ethane → propane + methane	−0.87	−2.34	−1.47	0.20	−1.67	98
3 ethane → butane + 2 methane	−1.69	−4.75	−3.06	0.41	−3.47	94
3 ethane → isobutane + 2 methane	−1.96	−6.52	−4.56	0.53	−5.09	96
4 ethane → pentane + 3 methane	−2.47	−7.14	−4.67	0.63	−5.30	91
4 ethane → isopentane + 3 methane	−1.44	−8.49	−7.05	0.72	−7.78	81
4 ethane → neopentane + 3 methane	−2.64	−11.93	−9.29	0.86	−10.16	96
5 ethane → cyclopentane + 5 methane	2.13	−3.69	−5.82	0.92	−6.73	73
6 ethane → cyclohexane + 6 methane	−4.43	−12.62	−8.19	1.13	−9.33	87
Branching Equations						
butane→ isobutane	−0.27	−1.77	−1.50	0.11	−1.61	90
pentane→ isopentane	1.02	−1.36	−2.38	0.10	−2.48	58
pentane → neopentane	−0.17	−4.79	−4.62	0.24	−4.86	92
isopentane→ neopentane	−1.20	−3.44	−2.24	0.14	−2.37	96

[a] $\Delta E^{(2)}$ is the total change in correlation energy, and $\Delta e^{(2)}_{intra}$ and $\Delta e^{(2)}_{inter}$ are the changes in the sum of intrapair and interpair energies, respectively. The percent of the total interpair stabilization of the products due to 1,4-interpair energies is given in the rightmost column. Both the HF and the MP2 energy changes (kcal/mol, cc-pvTZ basis set) are based on the MP2/cc-pVTZ geometries.

Table 2-3. LMO-MP2 decomposition of the correlation contribution ($\Delta E^{(2)} = \Delta E_{MP2} - \Delta E_{HF}$) to the electronic energy change of selected isodesmic and isomerization equations of simple alkanes.[a]

The isomerization of pentane to isopentane also is interesting. In this case increased 1,4-interpair stabilization accounts for only 58% of the total electron correlation stabilization of isopentane, while the rest results from remarkably large 1,5-pair correlations in isopentane. These large 1,5-pair contributions are due to the gauche interaction between isopentane's 1,4-methyl groups,

which causes crowding between the neighboring 1,6-hydrogen atoms (whose distances resemble those typical of hydrogens in 1,3- methyl groups, see Figure 4) and increased 1,5-C−H/C−H pair energies.

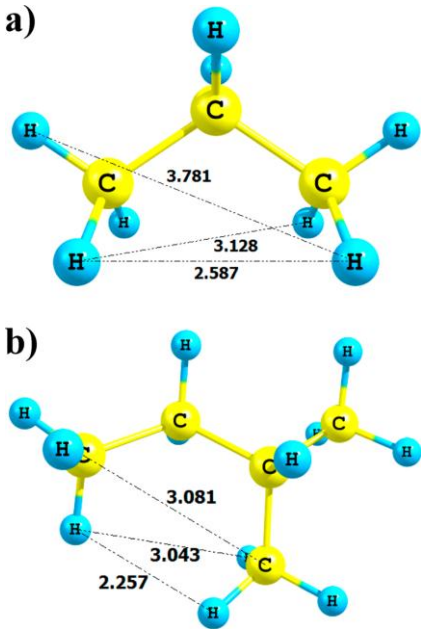

Figure 2-4. Selected distances (Å) between 1,5-hydrogens in propane and 1,6-hydrogens and 1,4-carbons in isopentane at the MP2/ccpVTZ level.

On the basis of our LMO-MP2 analysis, it is clear that 1,3-alkyl−alkyl electron correlation effects stabilize protobranchedalkanes considerably. But are such interactions "attractive"? Simple vdW considerations are suggestive. In our alkane set, most 1,4-pairs correspond to correlation effects between the C−H bonds in 1,3-alkyl groups. The shortest distances between the 1,5-hydrogen atoms involved in these 1,3-alkyl−alkyl interactions are about 2.59 Å (see Figure 4a). This value exceeds twice the sum of the various estimates for the

vdW radius of hydrogen given by Bondi,[52] Rowland and Taylor,[53] and Truhlar et al. (1.2 Å),[54] as well as that of Badenhoop and Weinhold (1.26−1.31 Å),[40] and Pauling (1.29 Å).[55] Hence these contacts are expected to be stabilizing. Aside from 1,5-C− H/C−H pairs, a smaller number of 1,5-C−H/C−C and C−C/ C−C pair energies also contribute to the enhanced stability of protobranched alkanes whose carbon chain lengths are long enough to accommodate such interactions. However the 1,5 H/ C and C/C distances of typical alkanes are generally also greater than the sum of their respective vdW radii (2.9 and 3.4 Å), so an attractive potential is expected.

Several recent investigations which attribute "attractive" character to the ∼2.6−3.1 Å 1,5 H/H interactions in hydrocarbons are also noteworthy. Tsuzuki et al.'s[56] analysis of dispersion interactions in n-alkane dimers revealed surprisingly strong association energies, −2.80, −3.57, and −4.58 kcal/mol for n-butane, n-pentane, and n-hexane dimers, respectively, as well as intermolecular H···H contact distances ranging from 2.407 to 3.625 Å, which are like the 1,5-H/H distances in propane. Shaik et al.'s[57] QTAIM study of the binding of methane and polyhedrane dimers attributed the stabilization of these species to their short H/H contacts in the 2.15−3.20 Å range. Yang and co-workers'[58] noncovalent interaction (NCI) analysis, which identifies stabilizing or destabilizing through space interactions based on the electron density topology of a molecule, found the 1,5-H/H interactions in hexamethylethane to be attractive. Finally Schreiner et al.[23] attributed the remarkable thermal stability of coupled diamondoid molecules subject to extreme steric crowding to attractive intramolecular H/H interactions in the 1.9−2.6 Å range and speculated that a similar H/H attractions might explain the origin of protobranching stabilization. Our own findings provide a basis for this hypothesis.

If the interactions between hydrogen atoms in 1,3-alkyl groups are indeed attractive, a caveat regarding 1,4-alkyl−alkyl interactions is warranted. Gauche 1,4-alkyl−alkyl interactions force short H/H and C/C contacts which are smaller than the sum of their combined vdW radii. This leads to intramolecular repulsion,[18c] as is evidenced by, for example, the lowered branching energy of isopentane relative to isobutane. Both isoalkanes contain one more protobranch than their linear isomers, but the energy difference between n-pentane and isopentane is smaller than that between n-butane and isobutane (1.77 vs 1.36 kcal/mol, MP2/cc-pVTZ electronic energies, see Table 3). This can be explained by repulsive interactions in isopentane between a pair of 1,6-hydrogen atoms and 1,4-carbon atoms, whose interatomic distances are less than the sum of their combined vdW radii (2.26 and 3.08 Å vs 2.40 and 3.40 Å, respectively). Hence only a portion of the electron correlation stabilization of isopentane relative to pentane is attributable to branching stabilization (about 58%, see Table 3), while the remaining correlation energy counteracts the overly repulsive vdW potential of the isopentane gauche interaction given by HF theory.

The HF vs MP2 energy difference between anti and gauche n-butane conformations, both of which have two protobranches, also is illustrative. HF theory overestimates the (electronic) energy difference of the two conformers, giving 1.14 kcal/mol, but the MP2/cc-pVTZ value of 0.56 kcal/mol agrees well with the high level ab initio estimate of Allinger et al., 0.62 kcal/mol.[59] In this case about 80% of the MP2 electron correlation stabilization of gauche n-butane is due to pair correlation effects contained in its 1,4-methyl−methyl interaction. However, as in isopentane, the 1,4-methyl−methyl interaction in gauche n-butane forces a pair of 1,6-hydrogen and 1,4-carbon atoms to distances (2.29 Å and 3.11 Å, respectively) shorter than the sum of their combined vdW radii; hence the correlation stabilization of gauche relative to anti n-butane does

not represent an attractive interaction. We note that large, highly branched alkane isomers have many gauche interactions, and these are likely to play a significant role in determining their relative stabilities.[60]

2.4 CONCLUSIONS

Electron correlation effects contribute strongly to both branching and protobranching stability. Isomerization and isodesmic evaluations of branching and protobranching stabilization tend to balance short-range correlation, while unbalanced long-range contributions usually are negligible. Unbalanced medium range effects are primarily responsible for the correlation stabilization of both branched and protobranched alkanes. This medium range correlation is due to 1,3-alkyl−alkyl interactions, or more precisely the 1,4-electron pair correlations contained in these interactions. Most 1,4-pair energies correspond to correlations between the C−H bonds in 1,3-alkyl moieties, and simple vdW considerations of the 1,5-H/ H distances involved suggest these interactions might be viewed as “attractive”.

2.5 METHODS

All geometry optimizations and harmonic frequency computations at the HF and MP2 levels were performed using the Gaussian 2009 program. Molecular surface area calculations were performed in Chimera[47] with $\rho = 0.001$. LMO-MP2 pair energies and B3LYP and B3LYP-D3 energies and harmonic frequencies were computed in GAMESS (version 2009).

2.6 REFERENCES

(1) Rossini, J. J. *Res. Natl. Bur. Stand.* **1934**, *13*, 21.

(2) Nenitzescu, C. D.; Chicos, I. *Ber. Dtsch. Chem. Ges.* **1935**, *68B*, 1584.

(3) Deitz, V. J. *Chem. Phys.* **1935**, *58*, 436.

(4) Syrkin, Y. K.; Dyatkina, M. E. *Structures of Molecules and the Chemical Bond*; Interscience Publishers: New York, **1950**; 243.

(5) Platt, J. R. *J. Phys. Chem.* **1952**, *56*, 328.

(6) Brown, R. D. *J. Chem. Soc.* **1953**, 2615.

(7) (a) Dewar, M. J. S.; Pettit, R. *J. Chem. Soc.* **1954**, 1625. (b) Dewar, M. J. S. *J. Am. Chem. Soc.* **1984**, *106*, 669.

(8) Pitzer, K. S.; Catalano, E. *J. Am. Chem. Soc.* **1956**, *78*, 4844.

(9) (a) Allen, T. L. *J. Chem. Phys.* **1959**, *31*, 1039. (b) Allen, T. L. *J. Chem. Phys.* **1965**, *43*, 4472.

(10) Pople, J. A.; Santry, D. P. *Mol. Phys.* **1964**, *7*, 269.

(11) Jacob, E. J.; Thompson, H. B.; Bartell, L. S. *J. Chem. Phys.* **1967**, *47*, 3736.

(12) Wiberg, K. B.; Bader, R. F. W.; Lau, C. D. H. *J. Am. Chem. Soc.* **1987**, *109*, 1001.

(13) (a) Laidig, K. E. *J. Phys. Chem.* **1991**, *95*, 7709. (b) Laidig's Hartree−Fock treatment has been criticized since it did not fully reproduce branching stability (see ref 18a), but re-computation of his data at the MP2 level does not alter his conclusions.

(14) (a) Ma, J.; Inagaki, S. *J. Am. Chem. Soc.* **2001**, *123*, 1193. (b) Inagaki, S. *Top. Curr. Chem.* **2009**, *289*, 83.

(15) Smith, D. W. *Phys. Chem. Chem. Phys.* **2001**, *435*, 44.

(16) Lee, M. C. J.; Smith, D. W. *Thermochim. Acta*. **2005**, *3*, 3562.

(17) (a) Wodrich, M. D.; Wannere, C. S.; Mo, Y.; Jarowski, P. D.; Houk, K. N.; Schleyer, P. v. R. *Chem. Eur. J.* **2007**, *13*, 7731. (b) Wodrich, M. D.; Schleyer, P. v. R. *Org. Lett.* **2006**, *8*, 2135. (c) Schleyer, P. v. R.; McKee, W. C. *J. Phys. Chem. A* **2010**, *114*, 3731. (d) Wodrich, M. D.; McKee, W. C.; Schleyer, P. v. R. *J. Org. Chem.* **2011**, *76*, 2439.

(18) (a) Gronert, S. *J. Org. Chem.* **2006**, *71*, 1209. (b) Gronert, S. *Org. Lett.* **2007**, *9*, 2211. (c) Gronert, S. *Chem. Eur. J.* **2009**, *15*, 5372.

(19) Estrada, E. *Chem. Phys. Lett.* **2008**, *463*, 422.

(20) Zavitsas, A. A.; Matsunaga, N.; Rogers, D. W. *J. Phys. Chem. A* **2008**, *112*, 5734.

(21) Ess, D. H.; Liu, S.; De Proft, F. J. *Phys. Chem. A* **2010**, *114*, 12952.

(22) Kemnitz, C. R.; Mackey, J. L.; Loewen, M. J.; Hargrove, J. L.; Lewis, J. L.; Hawkins, W. E.; Nielsen, A. F. *Chem. Eur. J.* **2010**, *16*, 6942.

(23) Schreiner, P. R.; Chernish, L. V.; Gunchenko, P. A.; Tikhonchuck, E. Y.; Hausmann, H.; Serafin, M.; Schlecht, S.; Dahl, J. E. P.; Carlson, R. M. K.; Fokin, A. A. *Nature* **2011**, *477*, 308.

(24) (a) Bartell, L. S. *J. Chem. Phys.* **1960**, *32*, 827. (b) Bartell, L. S. *J. Am. Chem. Soc.* **1959**, *81*, 3497.

(25) Redfern, P. C.; Zapol, P.; Curtiss, L. A.; Raghavachari, K. J. *Phys. Chem. A* **2000**, *104*, 5850.

(26) Grimme, S. *Angew. Chem., Int. Ed.* **2006**, *45*, 4460.

(27) Korth, M.; Grimme, S. *J. Chem. Theory Comput.* **2009**, *5*, 993.

(28) Wodrich, M. D.; Corminboeuf, C.; Schleyer, P. v. R. *Org. Lett.* **2006**, *8*, 3631.

(29) (a) Schreiner, P. R.; Fokin, A. A.; Pascal, R. A.; de Meijere, A. *Org. Lett.* **2006**, *8*, 83635. (b) Schreiner, P. R. *Angew. Chem. Int. Ed.* **2007**, *46*, 4217.

(30) Wodrich, M. D.; Corminboeuf, C.; Schreiner, P. R.; Fokin, A. A.; Schleyer, P. v. R. *Org. Lett.* **2007**, *9*, 1851.

(31) Lii, J.-H.; Allinger, N. L. *J. Mex. Chem. Soc.* **2009**, *53*, 96.

(32) Gao, H.; Bader, R. F. W.; Cortés-Guzmán, F. *Can. J. Chem.* **2009**, *87*, 1583.

(33) Grimme, S. *Org. Lett.* **2010**, *12*, 4670.

(34) Allinger, N. L. *Molecular Structure: Understanding Steric and Electronic Effects from Molecular Mechanics*; John Wiley and Sons Inc.: Hoboken, NJ, **2010**.

(35) Schwabe, T.; Huenerbein, R.; Grimme, S. *Synlett* **2010**, *41*, 1431.

(36) Shamov, G. A.; Budzelaar, P. H. M.; Schreckenbach, G. *J. Chem. Theory Comput.* **2010**, *6*, 477.

(37) (a) Song, J.-W.; Tsuneda, T.; Sato, T.; Hirao, K. *Org. Lett.* **2010**, *12*, 1440. (b) Song, J.-W.; Tsuneda, T.; Sato, T.; Hirao, K. *Theor. Chem. Acc.* **2011**, *130*, 851.

(38) Steinmann, S. N.; Wodrich, M. D.; Corminboeuf, C. *Theor. Chem. Acta* **2010**, *127*, 429.

(39) Bartell, L. S. J. *Phys. Chem. A* **2012**, *116*, 10460.

(40) (a) Badenhoop, J. K.; Weinhold, F. *J. Chem. Phys.* **1997**, *107*, 5406. (b) Badenhoop, J. K.; Weinhold, F. Int. *J. Quantum Chem.* **1999**, *72*, 269.

(41) The net methyl−methyl "attraction" (i.e. stabilization) is suggested by the pyramidal geometry of the tert-butyl radical, which contrasts with the planar preference of the parent methyl radical, see: Overill, R. E.; Guest, M. F. *Mol. Phys.* **1980**, *41*, 119.

(42) (a) Scott, D. W. *Chemical Thermodynamic Properties of Hydrocarbons and related substances; U.S. Bureau of Mines Bulletin No. 666*; U.S. Government Printing Office: Washington, DC, **1974**. (b) The 0 K heat of formation value for cyclohexane (−20.03 kcal/ mol) was taken from the NIST Computational Chemistry Comparison and Benchmark Database (CCCBDB).

(43) Kreig, H.; Grimme, S. *Mol. Phys.* **2010**, *108*, 2655.

(44) Grimme, S..; Antony, J.; Ehrlich, S.; Krieg, J. *J. Chem. Phys.* **2010**, *132*, 154104.

(45) These errors are mainly due to the long range character of the D3 correction, which contrasts with the medium range nature branching and protobranching stabilization.[26,33] This problem can be overcome by re-parameterizing the damping function to include medium range effects. See: Wodrich, M. D.; Jana, D. F.; Schleyer, P. v. R.; Corminboeuf, C. *J. Phys. Chem. A* **2008**, *112*, 11495.

(46) (a) Karton, A.; Gruzman, D.; Martin, J. M. L. *J. Phys. Chem. A* **2009**, *113*, 8434. (b) Karton, A.; Gruzman, D.; Martin, J. M. L. *J. Phys. Chem. A* **2009**, *113*, 11974.

(47) Pettersen, E. F.; Goddard, T. D.; Huang, C. C.; Couch, G. S.; Greenblatt, D. M; Meng, E. C.; Ferrin, T. E. *J. Comput. Chem.* **2004**, *25*, 1605.

(48) Wiberg et al. recently performed a similar correlation energy partitioning to examine intramolecular dispersion in cis and trans-halopropenes, see: Wiberg, K. B.; Wang, Y. W; Petersson, G. A.; Bailey, W. F. *J. Chem. Theory Comput.* **2009**, *5*, 1033.

(49) (a) Pulay, P.; Saebo, S. *Theor. Chim. Acta* **1986**, *69*, 357. (b) Saebo, S.; Pulay, P. Annu. *Rev. Phys. Chem.* **1993**, *44*, 213.

(50) (a) Pipek, J.; Mezey, P. G. *J. Chem. Phys.* **1989**, *90*, 4916.

(b) Boys, S. F. *Rev. Mod. Phys.* **1960**, *32*, 296. (c) Montogmery, J. A., Jr.; Frisch, M. J.; Ochterski, J. W.; Petersson, G. A. *J. Chem. Phys.* **2000**, *112*, 6532. (d) Edmiston, C.; Ruedenberg, K. *Rev. Mod. Phys.* **1963**, *35*, 457.

(51) Johnson, E. R.; Contreras-Garcia, J.; Yang, W. *J. Chem. Theory Comput.* **2012**, *8*, 2676.

(52) Bondi, A. *J. Phys. Chem.* **1964**, *68*, 441.

(53) Rowland, R. S.; Taylor, R. *J. Phys. Chem.* **1996**, *100*, 7384.

(54) Mantina, M.; Chamberlin, A. A.; Rosendo, V.; Cramer, C. J.; Truhlar, D. G. *J. Phys. Chem. A* **2009**, *113*, 5806.

(55) Pauling, L. *The Nature of the Chemical Bond and the Structure of Molecules and Crystals*, 3rd ed.; Cornell University Press: Ithaca, NY, **1960**.

(56) Tsuzuki, S.; Honda, K.; Uchimaru, T.; Mikami, M. *J. Phys. Chem. A* **2004**, *108*, 10311.

(57) Echenerria, J.; Aullón, G.; Danovich, D.; Shaik, S.; Alvarez, S. *Nat. Chem.* **2011**, *3*, 323.

(58) Johnson, E. R.; Keinan, S.; Mori-Sánchez, P.; Contreras-Garcia, J.; Cohen, A. J.; Yang, W. *J. Am. Chem. Soc.* **2010**, *132*, 6498.

(59) Allinger, N. L.; Fermann, J. T.; Allen, W. D.; Schaefer, H. F., III. *J. Chem. Phys.* **1997**, *106*, 5143.

(60) Gonthier, J. F.; Wodrich, M. D.; Steinmann, S. N.; Corminoeuf, C. *Org. Lett.* **2010**, *12*, 3070.

CHAPTER 3

A HUCKEL THEORY PERSPECTIVE ON MOBIUS AROMATICITY

-W. C. McKee, J. I. Wu, H. S. Rzepa, P. v. R. Schleyer, 2013, Org. Lett., 15, 3432-3435,

3.1 ABSTRACT

Heilbronner's Hückel molecular orbital treatment of Möbius 4n-π annulenes is revisited. When uneven twisting in π-systems of small Möbius rings is accounted for, their resonance energies become comparable to iso-π-electronic linear alkenes with the same number of carbon atoms. Larger Möbius rings distribute π-twisting more evenly but exhibit only modest aromatic stabilization. Dissected nucleus independent chemical shifts (NICS), based on the LMO (localized molecular orbital)-NICS(0)π index confirm the magnetic aromaticity of the Möbius annulenes considered.

3.2 INTRODUCTION

In 1964, Edgar Heilbronner demonstrated that a model basis for a 4n π-electron annulene, consisting of a planar cyclic array of atomic p orbitals, could accommodate an evenly distributed 180^{o} twist without a loss in π-electron energy.[1a] Remarkably, he found that the normal Hückel rule was reversed for these twisted annulenes, with 4n π-electron species being closed shell and 4n + 2 species open shell. Heilbronner inscribed an unsigned[1b] representation of the twisted p orbital basis onto a Möbius strip and referred to these twisted species as "Möbius-type" annulenes. The term "Möbius aromaticity" was coined shortly afterward,[2] but further interest in the Möbius concept lay mostly dormant until 1998.[3]

Today interest in the Möbius aromaticity of 4n-π annulenes exhibiting a half twist in their π-system widespread.[4,5] Many such species have been characterized computationally,[6,7] but their experimental detection has been problematic. A Möbius conformation of the [9]annulene cation was postulated to exist as a short-lived intermediate upon solvolysis of exo-9-chlorobicylco[6.1.0]nona-2,4,6-triene and 9-chlorocyclononatetraene,[3] but recent evidence indicates a Hückel (untwisted) structure is more likely.[8] Herges et al. reported synthesis of the first Möbius annulene in 2006,[9] but its aromaticity has been contested.[10]

Ab initio computations on the neutral 4n-π [12]-, [16]-, and [20]annulenes suggest that their lowest lying Hückel conformers are all more stable than any Möbius topology.[6a] Moreover, these species exhibit small barriers to *cis-trans* isomerization;[11] hence, experimental isolation of neutral Möbius annulenes seems unlikely. Möbius conformations of a few annulene cations are believed to exist as global minima, but most undergo fast exothermic electrocyclization,[7] and none have been observed experimentally.

The difficulties in detecting Möbius aromatic annulenes may seem surprising since aromaticity is often associated with stability. Literature evaluations of Möbius annulene aromaticities have been based mainly on geometric and magnetic criteria, and the thermal and kinetic instability of these systems attributed to ring strain. But do "medium sized" Möbius [n]annulenes with 8, 12, 16, and 20 carbons benefit from aromatic stabilization? According to Heilbronner's simple Hückel molecular orbital (HMO) treatment, Hückel and Möbius conformations of 4n_π annulenes have the same resonance energy (RE).

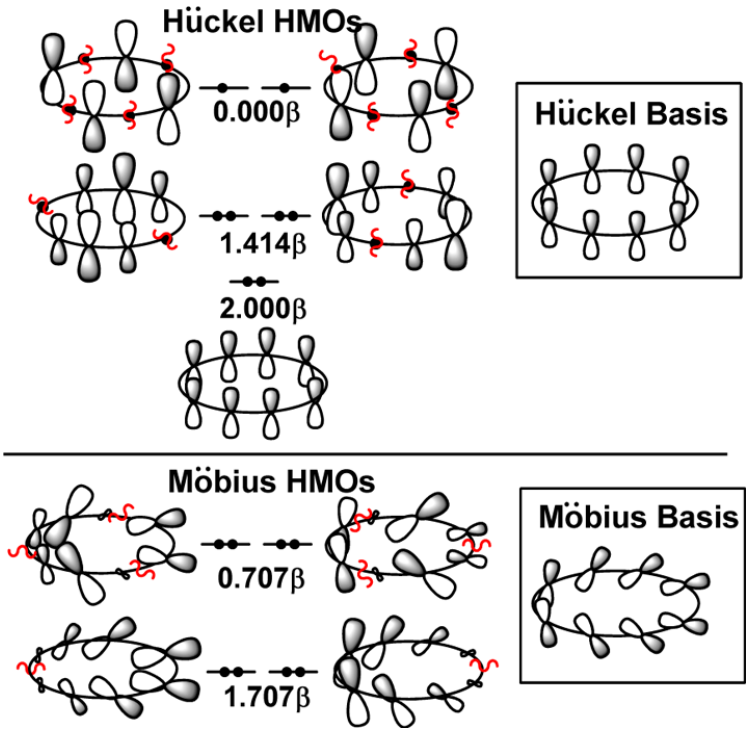

Figure 3-1. HMO bases and occupied symmetry orbitals for Hückel (top) and Möbius (bottom) cyclooctatetraene. Phase shifts are marked as red lines.

Zimmerman's[2] qualitative explanation of this result is that the π-electrons in 4n-π annulenes experience the same total number of phase shifts in their MOs, irrespective of whether the p orbital basis has Hückel or Möbius topology. For example, the four lowest energy π-electrons in both Hückel and Möbius cyclooctatetraene experience a sum total of four nodes between them and the next four a total of 12 (See Figure 1). Hence, as the REs of medium-sized Hückel 4n-π annulenes exceed those of a linear polyene reference with the same number of carbon atoms and π electrons,[12] it seems closed shell Möbius conformations should be stabilized energetically by aromaticity.

Of course, Heilbronner's HMO treatment was very simplistic. In reality, Möbius annulenes are not planar, and their bending distortion into three dimensions, characterized by writhe (W_r), results in unequal twist angles between adjacent p orbitals, which need not sum to π. Instead, it is the linking number (L_k) that must sum to π for half-twisted Möbius systems,[13] where $L_k = T_w + W_r$, and T_w is the sum of local p AO torsional angles. Importantly, depending on the value of W_r, T_w may be either less or greater than π, which can significantly impact computed HMO REs of Möbius annulenes. Other important consequences of nonplanarity include σ-π mixing (which results in σ→π* hyperconjugation)[14] and varying degrees of bond length alternation.[15]

In addition, the highest symmetry that a Möbius annulene can attain is C_2,[5] which has no degenerate representations. Hence, the quasi-π MOs of Möbius annulenes do not occur in degenerate pairs. The 2-fold MO degeneracy given by Heilbronner's treatment is an artifact of assuming that the HMO resonance integrals (β), which represent the interaction energy between two adjacent p AOs, are equal for all pairs of p orbitals. In reality, two βs will generally only be

equal if they are symmetry equivalent.[16] Moreover, Janneskens et al. have shown that interactions between non-adjacent p AOs, which are neglected in HMO theory, are also unequal for Möbius annulenes.[16] Hence, MO degeneracies are absent at the SCF level.

Despite its inherent simplicity, HMO theory's success in predicting the reversed rules for aromaticity in twisted 4n-π annulenes indicates its qualitative usefulness. Hence, an improved HMO treatment which takes explicit account for the non-uniform twist angles between each pair of adjacent p AOs may help explain the apparent lack of aromatic stabilization in medium sized Möbius annulenes.

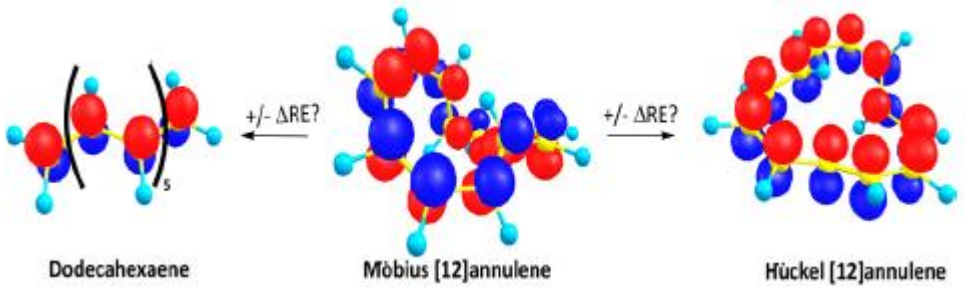

Figure 3-2. Pictorial representation of the natural hybrid orbital basis for the iso-π-electronic species dodecahexaene, and Möbius and Hückel [12]annulene.

To determine the twist angles between adjacent p orbitals in annulenes at the SCF level, we employ p-type natural hybrid orbitals (NHOs)[17] as our basis (see Figure 2 for pictorial representations). NHOs are "natural" in the sense that they exhibit the maximum occupancy possible for an orthonormal set of localized sp^n and p-type hybrid basis orbitals. Hence, p NHOs

conform as closely as possible to the HMO assumption that each carbon atom in a neutral annulene contributes one electron to the π-system via its p AO.[18a]

In a minimal basis, a twisted p NHO can be written as a linear combination of $2p_x$, $2p_y$, and $2p_z$ natural atomic orbitals (NAOs) as[18b]

$$\mathbf{h_p} = c_1\mathbf{p_x} + c_2\mathbf{p_y} + c_3\mathbf{p_z} \quad (1)$$

where $\mathbf{h_p}$ is a twisted p orbital and $c_{1\text{-}3}$ are its expansion coefficients in terms of untwisted $2p_x$, $2p_y$, and $2p_z$ NAOs. Since the "direction" of a Cartesian p NAO is that of a unit vector pointing in its Cartesian direction (i.e., a p_z orbital is directed along the z-axis) the same coefficients in (1) also define the direction of a twisted p NHO as.[17]

$$D(\mathbf{h_p}) = c_1\mathbf{x} + c_2\mathbf{y} + c_3\mathbf{z} \quad (2)$$

where $D(\mathbf{h_p})$ is the direction of the p orbital and $c_{1\text{-}3}$ its x, y, and z components. Once the directional vectors of all p NHOs are known, they can be placed on their respective carbon atoms, and the $D(\mathbf{h_p})_i$-C_i-C_j-$D(\mathbf{h_p})_j$ dihedral angle gives the twist angle (θ_{ij}) between the p orbitals on adjacent carbon atoms C_i and C_j. Substituting each θ_{ij} into the expression $\beta_{ij} = \cos(\theta_{ij})$ gives the resonance integrals between all adjacent p NHOs in a system, and the HMO REs of twisted annulenes can then be computed in the normal way.

3.3 METHODS

We evaluated the p NHO twist angles T_w and W_r for Möbius andHückel conformations of [8]-, [12]-, [16]-, and [20]annulene at the HF/6-31G*//B3LYP/6-311+G** level. The Möbius and Hückel geometries of [12]-, [16]-, and [20]annulene correspond to compounds **1**, **5**, **7**, **11**, **13**, and **14** in ref 6a. The Hückel structure of [8]annulene was taken to be tub-shaped D_{2d} cyclooctatetraene, and the Möbius conformer C_2 *cis*,*cis*,*cis*,*trans*-cyclooctatetraene from ref 16. We also computed the LMO-NICS(0)π magnetic metric of aromaticity[21] for each annulene at the PW91/IGLOIII //B3LYP/6-311+G**) level.

3.4 RESULTS AND DISCUSSION

The HMO REs for an idealized Heilbronner basis (i.e., no p twisting for Hückel conformers and a constant 180^o/n p orbital twist for Möbius [n]annulenes) and the unevenly twisted p NHO basis are tabulated in Table 1 as HMO RE_1 and HMO RE_2, respectively. The HMO REs of iso-π-electronic linear C_nH_{n+2} alkenes are also provided for comparison. For a neutral polyene with an even number of π-electrons, HMO REs are obtained by summing the energy of eachπ-electron to give the total π-electron energy of the system (Tπ-e) and then subtracting from this value *m* times the Tπ-e of ethylene, where *m* is the number of double bonds in the polyene. For example, the Tπ-e of benzene and ethylene are 8.00β and 2.00β, respectively, and the HMO RE of benzene is $8.00\beta - 3(2.00\beta) = 2.00\beta$.

The HMO parameter β carries units of energy; hence, in principle HMOREs in terms of β can be converted to more familiar energy units (e.g., kcal/mol). For example, if the RE of benzene is taken to be 60.0 kcal/mol, then β = 30.0 kcal/mol. In practice, however, the value of β

depends on the theoretical method or thermodynamic equation used to evaluate the RE of a given system. Thus, in order to remove indeterminacies associated in the value of β, we define an HMO RE ratio (HMORR) as the quotient of the HMO RE of a polyene with that of an iso-π-electronic linear polyalkene with the same number of carbon atoms. For example, the HMO RR of benzene is: (HMORE[benzene])/(HMO RE [hexatriene]) = 2.02. It is evident from the definition of HMO RR that values greater than 1 indicate aromatic stabilization (i.e., energetic aromaticity), and values less than 1 antiaromatic destabilization.

	C_8H_{10}	[8]annulene		$C_{12}H_{14}$	[12]annulene		$C_{16}H_{18}$	[16]annulene		$C_{20}H_{22}$	[20]annulene	
	l	*h*	*m*	*l*	*h*	*m*	*l*	*h*	*m*	*l*	*h*	*m*
HMO RE_1[a]	1.518β	1.657β	1.657β	2.592β	2.928β	2.928β	3.676β	4.109β	4.109β	4.763β	5.255β	5.255β
HMO RR_1[b]	1	1.092	1.092	1	1.130	1.130	1	1.118	1.118	1	1.103	1.103
HMO RE_2[c]	1.518β	1.125β	1.434β	2.592β	1.944β	2.495β	3.676β	3.497β	4.084β	4.763β	4.960β	5.103β
HMO RR_2[d]	1	0.741	0.945	1	0.750	0.963	1	0.951	1.111	1	1.041	1.071
avg θ[e]	0	18.41	17.33	0	19.18	15.88	0	9.97	9.73	0	6.31	8.29
std dev θ[f]	0	18.41	22.08	0	18.55	14.56	0	10.53	6.49	0	7.40	7.59
T_w[g]		0.000	−0.863		0.104	−1.462		0.000	−0.244		−0.007	−0.725
W_r[g]		0.000	−0.137		−0.104	0.462		0.000	−0.756		0.007	−0.275
NBO RR[h]	1	0.625	0.944	1	0.678	1.062	1	0.925	1.917	1	0.992	1.143
rel *E*[i]		0.00	+21.37		0.00	+4.16		0.00	+15.12		0.00	+6.75
$NICS(0)_\pi$[j]		−3.80	−9.87		+4.44	−11.08		+10.10	−11.73		+12.49	−9.00

[a] HMO RE_1 = HMO resonance energy (RE) for an evenly twisted (Heilbronner) p orbital basis. [b] HMO RR_1 = RE ratio, quotient of the RE of a species the RE a linear alkene with the same number of π-electrons and carbon atoms (using an evenly twisted p basis). [c] HMO RE_2 = HMO RE for an unevenly twisted p NHO basis (HF/6-31G*//B3LYP/6-311+G**). [d] HMO RR_2 = RE ratio for an unevenly twisted p NHO basis. [e] Avg θ = average of the unsigned p NHO twist angles (deg). [f] Standard deviation of the unsigned p NHO twist angles (deg). [g] Twist and writhe values (in units of π) are based on p NHO directional vectors and B3LYP/6-311+G** geometries. [h] NBO RR_2 = NBO π-electron RE ratio. [i] Rel *E* = relative electronic energy (kcal/mol) at B3LYP/6-311+G**. [j] LMO-$NICS(0)_\pi$ chemical shifts (ppm) (PW91/IGLOIII//B3LYP/6-311+G**).

Table 3-1. Twist (T_w), writhe (W_r), and HMO, NBO, and LMO-$NICS(0)_\pi$ π-electron delocalization data for selected linear (*l*) and cyclic Hückel (*h*) and Möbius (*m*) polyenes.

The most striking feature of the HMO RR_1 values in Table 1 is that they are all nearly equal to 1. Hence, even under idealized Heilbronner-type assumptions, the REs of medium-sized

Möbius and Hückel annulenes are nearly the same as those of their corresponding iso-π-electronic linear polyene. The HMO REs and RRs all decrease when uneven p twisting is accounted for (see HMO RE_2 and HMO RR_2 in Table 1). The decreases are most severe for smaller rings and affect Hückel conformers more than their Möbius counterparts. The HMO RE_2 and RR_2 values depend not only on the value of T_w, but also on the magnitude of each individual p orbital twist angle, and how evenly the total amount of p twisting is distributed throughout the ring.[13] These factors can be qualitatively understood in terms of the average and standard deviation of the unsigned p orbital twist angles in each ring system (see Avg. θ and Std. Dev. θ in Table 1).

The HMO REs of Hückel 4n-π annulenes are maximized when all p orbital twist angles are equal to zero. Hence their distortion into three dimensions (which relieves open shell instability) lowers their REs more than for Möbius isomers where some p twisting in natural. In general the amount of p twisting decreases, and is distributed more evenly as ring size increases (see avg θ and std dev θ in Table 1). Thus, the smaller Hückel [8]- and [12]annulenes have HMO RR_2 values significantly less than 1, while the values for the 16- and 20-membered rings are nearly equal to 1. This suggests that large 4n-π Hückel annulenes should behave like linear polyenes.

The HMO RR2 values for Möbius conformations are all close to 1 and increase slightly as the rings become larger, allowing their avg θ and std dev θ values to decrease. HMO RR_2 is largest for Möbius [16]annulene, but its HMO RE_2 is only 1.111 times as large as that of linear $C_{16}H_{18}$. These results suggest that medium-sized Möbius annulenes are not stabilized by π-aromaticity to any significant degree.

Our simple HMO treatment takes no account of bondlength alternation, the tilting of p orbitals toward or away from one another, and the weak interactions between non-adjacent p orbitals. The computed annulene NBO RR values gauged the importance of these effects. The NBO RR values are defined in the same way as HMO RRs but are based instead on the quotient of NBO π-REs. Table 1 reveals the qualitative agreement of the NBO RR with the HMO RR2 values. The smaller Hückel annulenes exhibit NBO RRs significantly less than 1, whereas the Möbius NBO RR_2s are generally close to unity. Möbius [16]annulene is an exception. It projects most of its twisting strain into writhe, and its NBO RR, 1.917, is considerably larger than unity. For the reasons stated above, the NBO RR values are probably more accurate than HMO RR2s. However, the NBO RR of Möbius [16]annulene is still considerably smaller than the corresponding 3.220 benzene value.

Dissected localized molecular orbital (LMO)[19] nucleus independent chemical shifts (NICS),[20,21] NICS(0)π, computed at the heavy atom center of each of the Möbius/Hückel rings, including contributions only from the "π" LMOs, confirm that Möbius cycles follow the reversed Hückel π electron count rule for aromaticity. As shown in Table 1, the Hückel [4n]annulenes display negligibly small negative to modestly positive NICS(0)π values, indicative of non-aromaticity to weak antiaromaticity.[22] Conversely, the Möbius conformations exhibit negative NICS(0)π values ranging from −9.00 to −11.73 ppm, about half of the −23.89 ppm benzene value, indicating modest π aromaticity. Hence, energetic and magnetic aromaticity metrics contrast for 4n-π annulenes. Such disparate evaluations for Hückel conformers were noted previously by Wannere et al.,[15a] and our present analysis suggests a similar situation holds for Möbius cycles, which are aromatic by magnetic, but not energetic, criteria. However, even if the

REs of Möbius annulenes are not much greater than those of their corresponding linear iso-π-electronic polyene analogues, the notion that the RE of a twisted π system can rival that of an untwisted arrangement is nonetheless remarkable.

3.5 REFERENCES

(1) (a) Heillbronner, E. *Tetrahedron Lett.* **1964**, 1923. (b) Note, however, that Heilbronner's derivation of the rules for Möbius aromaticity necessarily included signed p AOs.

(2) Zimmerman, H. E. *Acc. Chem. Res.* **1971**, *4*, 272.

(3) (a) Mauksch, M.; Gogonea, V.; Jiao, H.; Schleyer, P. v. R. *Angew. Chem, Int. Ed.* **1998**, *37*, 2395.

(4) Rzepa, H. S. *Chem. Rev.* **2005**, *105*, 3697.

(5) Herges, R. *Chem. Rev.* **2006**, *106*, 4820.

(6) (a) Castro, C.; Isborn, C. M.; Karney, W. L.; Mauksch, M.; Schleyer, P. v. R. *Org. Lett.* **2002**, *4*, 3413. (b) Mauksch, M.; Tsogoeva, S. B. *Chem. Eur. J.* **2010**, *16*, 7843. (c) Zhu, C.; Li, S.; Luo, M.; Zhou, X.; Niu, Y.; Lin, M.; Zhu, J.; Cao, Z.; Lu, X.; Wen, T.; Xie, Z.; Schleyer, P. v. R.; Xia, H. *Nature Chem.* **2013** (DOI:10.1038/NCHEM.1690).

(7) Mucke, E.-K.; Schönborn, B.; Köhler, F.; Herges, R. *J. Org. Chem.* **2011**, *76*, 35.

(8) Bucher, G.; Grimme, S.; Huenerbein, R.; Auer, A. A.; Mucke, E.; Kohler, F.; Siegwarth, J.; Herges, R. *Angew. Chem. Int. Ed.* **2009**, *48*, 9971.

(9) Ajami, D.; Hess, K.; K€ohler, F.; Nather, C.; Oeckler, O.; Simon, A.; Tamamoto, C.; Okamoto, Y.; Herges, R. *Chem. Eur. J.* **2006**, *12*, 5434.

(10) Castro, C.; Chen, Z.; Wannere, C. S.; Jiao, H.; Karney, W. L.; Mauksch, M.; Puchta, R.; Hommes, N. J. R. v. E.; Schleyer, P. v. R. *J. Am. Chem. Soc.* **2005**, *127*, 2425.

(11) Castro, C.; Karney, W. L. *J. Phys. Org. Chem.* **2012**, *25*, 612.

(12) Kutzelnigg, W. *J. Comput. Chem.* **2006**, *28*, 25.

(13) (a) Rappaport, S. M.; Rzepa, H. S. *J. Am. Chem. Soc.* **2008**, *130*, 7613. (b) Wannere, C. S.; Rzepa, H. S.; Rinderspacher, C.; Ankan, P.; Allan, C. S. M.; Schaefer, H. F., III; Schleyer, P. v. R. *J. Phys. Chem. A.* **2009**, *113*, 11619.

(14) McKee, W. C.; Wu, J. I.; Hofmann, M.; Berndt, A.; Schleyer, P. v. R. *Org. Lett.* **2012**, *14*, 5712.

(15) (a) Wannere, C. S.; Moran, D.; Allinger, N. L.; Hess, B. A., Jr.; Schaad, L. J.; Schleyer, P. v. R. *Org. Lett.* **2003**, 5, 2983. (b) Wannere, C. S.; Sattelmeyer, K. W.; Schaefer, H. F., III; Schleyer, P. v. R. *Angew. Chem. Int. Ed.* **2004**, *43*, 4200.

(16) Havenith, R. W. A.; Lenthe, J. H. v.; Janneskens, L. W. *Int. J. Quantum Chem.* **2001**, *85*, 52.

(17) Weinhold, F.; Landis, C. *Valency and Bonding, A Natural Bond Orbital Donor-Acceptor Perspective*; Cambridge University Press: Cambridge, **2005**.

(18) (a) For our annulene set the average p NHO occupancies are ≥ 0.996e. (b) In a non-minimal basis p NAOs with higher quantum number n (e.g., 3p, etc.) have a negligible effect on the p NHO direction (see ref 17, pp 107_110).

(19) Schleyer, P. v. R.; Manoharan, M.; Wang, Z. X.; Kiran, B.; Jiao, H.; Puchta, R.; Hommes, N. J. R. v. E. *Org. Lett.* **2001**, *3*, 2465.

(20) Schleyer, P. v. R.; Maerker, C.; Dransfeld, A.; Jiao, H. J.; Hommes, N. J. R. v. E. *J. Am. Chem. Soc.* **1996**, *118*, 6317.

(21) Chen, Z. F.; Wannere, C. S.; Corminboeuf, C.; Puchta, R.; Schleyer, P. v. R. *Chem. Rev.* **2005**, *105*, 3842.

(22) An alternative analysis of the ring currents of medium-sized Möbius annulenes is presented in refs 5 and 7.

CHAPTER 4

WHY DO TWO π-ELECTRON FOUR MEMBERED RINGS PUCKER?

-W. C. McKee, J. I. Wu, M. Hofmann, A. Berndt, P. v. R. Schleyer, 2012, Org. Lett., 14, 5712-5715, Reprinted here with permission of publisher.

4.1 ABSTRACT

Notwithstanding their two (i.e., 4n + 2) π electrons, the cyclobutadiene dication and related isoelectronic derivatives favor puckered geometries, despite the reduction in vicinal π overlap and in their ring atom bond angles. This non-planar preference is due to σ → π* hyperconjugative interactions across the ring rather than to partial 1,3-bonding. Electronegative substituents (e.g., F in $C_4F_4^{2+}$) reduce the σ → π* electron delocalization, and planar geometries result. In contrast, electropositive groups (e.g., SiH_3 in $C_4(SiH_3)_4^{2+}$) enhance hyperconjugation and increase the ring inversion barriers substantially.

4.2 INTRODUCTION

Although expected to be planar due to two π electron Hückel aromaticity, maximum vicinal π-overlap, and the decrease in the already small bond angles, four-membered rings (4MRs) such as **1a**-**4a** (see Figure 1) are puckered.[1] Following Olah's success in preparing, inter alia, the persistent tetramethylcyclobutadiene dication,[1f] theoretical computations predicted that $C_4(CH_3)_4^{2+}$ along with the **1a**,[1b,2a,b] **2a**,[2a,b,c] and **4a**[1a] prototypes favored non-planar geometries (see Figure 1). These computations were subsequently verified by comparison of experimental and computed chemical shifts of the $C_4(CH_3)_4^{2+}$,[1c] as well as X-ray structure determinations of **2a**-**4a** derivatives.[3-5]

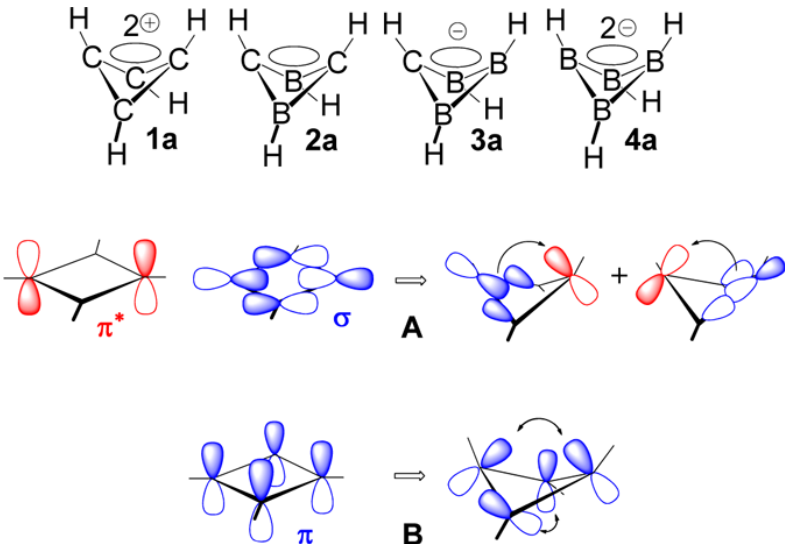

Figure 4-1. Pictorial depiction of **1a**-**4a**, and the σ→π* cross-ring hyperconjugation and partial 1,3 p-p bonding mechanisms invokes to explain their puckered ring structures.

Such ring puckering was first attributed to σ and π*orbital mixing in lower symmetry; hyperconjugation results (see A in Figure 1).[1b,2a] Increased 1,3 p-orbital overlap and double homoallylic bonding upon folding (see B)[2] were proposed as an alternative.[2h,g] This is akin to the homoaromaticity generally invoked for the cyclobutenyl cation (i.e., the homocyclopropenylium ion) and similar systems.[6]

4.3 RESULTS AND DISCUSSION

Does hyperconjugation (A) or enhanced 1,3-bonding (B) stabilize the folded conformers of non-planar **1a**-**4a**? Does puckering influence the aromaticity of these 4MRs with two quasi "π" electrons? Irngartinger found no significant experimental support for 1,3-interactions in $(CH)_2(BNR_2)_2$ (R = isopropyl).[3c] Firme et al.'s evidence for increased electron densities at the ring centers of non-planar derivatives of **1a**[7] is not decisive. As both hyperconjugation and partial 1,3-bonding might delocalize the electron density upon puckering, their relative importance is uncertain.

Other 4MRs with electron-deficient tricoordinate centers, e.g., the cyclobutyl cation and cyclobutylidene, also prefer non-planar geometries.[8,9] Even B_4H_4 (**5a*** and **5a**, Figure 2 top) has a low energy D_{2d} conformer strongly stabilized (by 39 kcal/mol) relative to its planar D_{4h} form. Since the B_4H_4 ring has four tricoordinate centers, but no π-electrons, the puckering preference must be due to changes in the σ-skeleton. Indeed, correlation of the delocalized Kohn-Sham MOs (Figure 2 top, HOMO − 1s: $e_u \rightarrow e$) demonstrates that the B-B σ-bonding orbitals (analogous to the σ-orbital depicted in A of Figure 1) become lower in energy upon puckering. This supports the hyperconjugation argument. NBO localization of the canonical molecular

orbitals (CMOs) confirms that ring folding reduces the B-B σ-bond occupancies of **5a** (by 0.08 electrons) compared to those of **5a***, while the formally empty p-orbitals in **5a*** gain 0.12 electrons each in **5a**, due to σ → π* hyperconjugation.

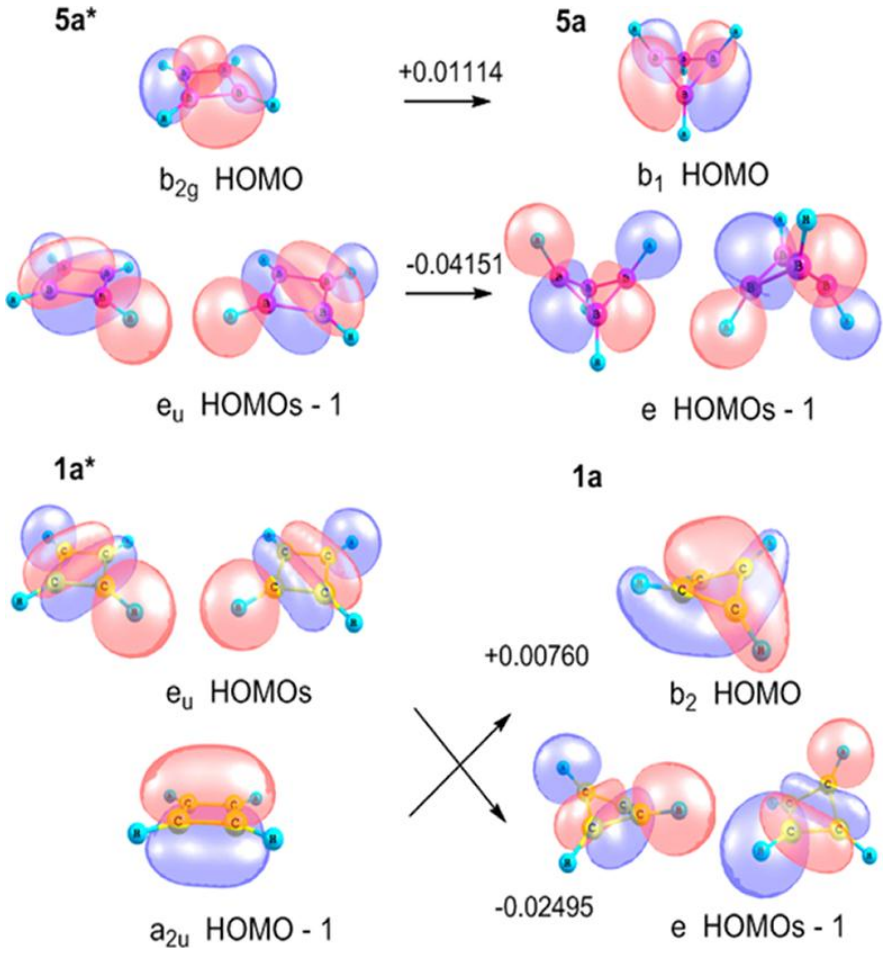

Figure 4-2. B3LYP/6-311+G** changes in orbital energies (a.u.) upon puckering for B_4H_4 (**5a*** → **5a**, top) and for $C_4H_4^{2+}$ (**1a*** → **1a**, bottom). The σ-orbital energies of non-planar forms are lowered, but the π HOMO−1 energy of **1a*** is raised. Hence, π-orbital changes alone cannot be the cause of puckering.

Likewise, the degenerate σ-MOs (HOMOs, e_u) of **1a*** are lowered upon puckering to **1a** (HOMO − 1s, e) (see Figure 2, bottom), while the π-orbital energies are raised. This refutes the possibility of any 1,3-bonding being responsible for the non-planarity of these 4MRs with two quasi "π" electrons. The corresponding orbital energy changes of **2a**-**4a** are similar. Upon puckering, the stabilizing 2π electron delocalization in planar **1a*** is reduced to two weaker 1,3-π orbital interactions in **1a** (see the b_2 orbital in Figure 2, bottom and the discussion below). As depicted for **1a** in Figure 3a, the σ-NBO occupancies of **1a**-**4a** also are lowered (e.g., by 0.03 electrons for each C-C σ bond in $C_4H_4^{2+}$), while the p* occupancies of the ring atoms are raised (0.03e for each C p* orbital of $C_4H_4^{2+}$). A second order NBO perturbation analysis of the NBO Fock matrix confirms that hyperconjugative interactions between these orbitals (see Figure 2a) are responsible for this charge transfer. Moreover, the magnitude of the σ → p* hyperconjugation in 1a-4a increases in the same order as their energetic puckering preferences (see Figure 4).

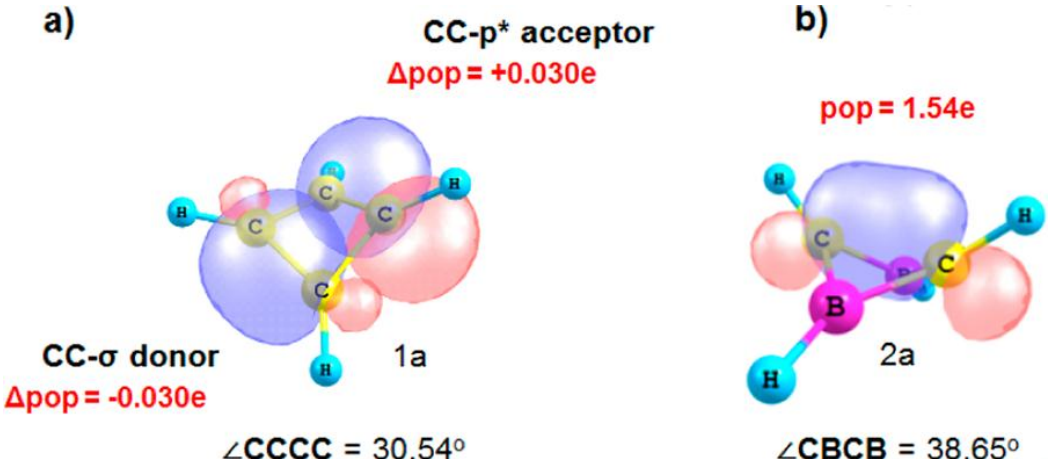

Figure 4-3. (a) Schematic depiction of the σ → p* cross-ring hyperconjugative interactions responsible for puckering in **1a**. (b) The partly occupied 1,3 C-C NBO for puckered **2a**.

In the NBO formalism, the magnitude of hyperconjugative stabilization between a donor-acceptor localized orbital pair (i,j) is proportional to the square of their off diagonal Fock matrix elements (F_{ij}), and inversely proportional to their orbital energy difference ($e_i - e_j$). The F_{ij} term corresponds roughly to the degree of orbital "mixing" and can be related to the overlap of the pre-orthogonal (i.e., overlap allowed) donor-acceptor orbital pair via a Mulliken-type approximation.[10] This overlap is zero in the planar conformations of **1a-4a**, but puckering introduces overlap of the σ and p* ring orbitals (see Figure 3a) giving rise to cross-ring hyperconjugative stabilization.

Cross-ring hyperconjugation is also facilitated by the small $e_i - e_j$ energy gaps arising from angle strain. In **1a**-**4a** the $e_i - e_j$ values vary from 0.35 to 0.57 a.u., i.e., on the low end of the 0.28-1.52 au $e_i - e_j$ range typically observed for donor-acceptor interactions.[11] In addition to its inherent stabilizing character, hyperconjugation also lowers the occupancies of the strained ring σ-bond orbitals, and thus reduces their mutual interelectronic repulsion. Consequently, the fact that the σ-HOMO energies of **1a*** lie above its π-orbital energy indicates high strain (see Figure 2, bottom). The opposite CMO order in **1a** indicates a decrease of this strain upon puckering.[12]

Substituent effects confirm the importance of cross-ring hyperconjugation on the geometries of the **1a**-**4a** analogs. Electronegative groups deactivate σ → π* hyperconjugation and favor planar geometries (indeed, computations found $C_4F_4^{2+}$, **1b** to be planar as early as

1978).[1b] The F substituted **2b**-**4b** analogs also prefer planarity considerably. The strong σ-electron withdrawal by F, evident from Natural Population Analyses (NPA),[13,14] reduces the donor strength of the ring σ-bonds significantly.

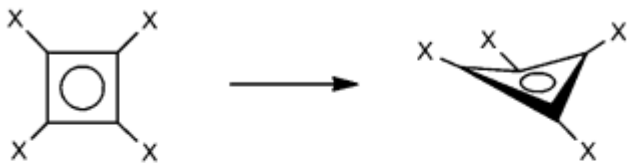

X =	**a** (H)	**b** (F)	**c** (SiH_3)
1 ($C_4X_4^{2+}$)	-8.37	+15.03	-22.72
2 ($C_2B_2X_4$)	-17.24	+13.86	-26.11
3 ($CB_3X_4^-$)	-11.77	+11.40	-19.53
4 ($B_4X_4^{2-}$)	-12.42	+10.54	-21.34

Figure 4-4. B3LYP/6-311+G** energy changes (kcal/mol) upon puckering for **1a**-**4a** and their F (**1b**-**4b**) and SiH_3 (**1c**-**4c**) substituted derivatives. The X = F estimates were based on partially optimized geometries with ring puckering angles fixed at the corresponding X = H values.

Electropositive substituents have the opposite effect. The inductive electron donation of SiH_3 groups to the ring σ-bonds[15,16] of **1c**-**4c** enhances σ → π* hyperconjugation and elevates the inversion barriers substantially (see Figure 4). Carbenic 4MR-2π e-aromatic species also may be employed for isoelectronic substitutions of a CH(+) by a singlet C:. Indeed, such carbene species strongly prefer puckered conformations (e.g., by 41.6 kcal/mol for C_4H_2; see Figure 5), due to

the greatly enhanced cross-ring hyperconjugative interactions and the lowered occupancy of their strained C-C σ bonds. Such substituent effects agree with previous structural studies on **1a** derivatives[1b,7] and support the hyperconjugation rationale for the puckering of 4MR-2π e- aromatic systems impressively.

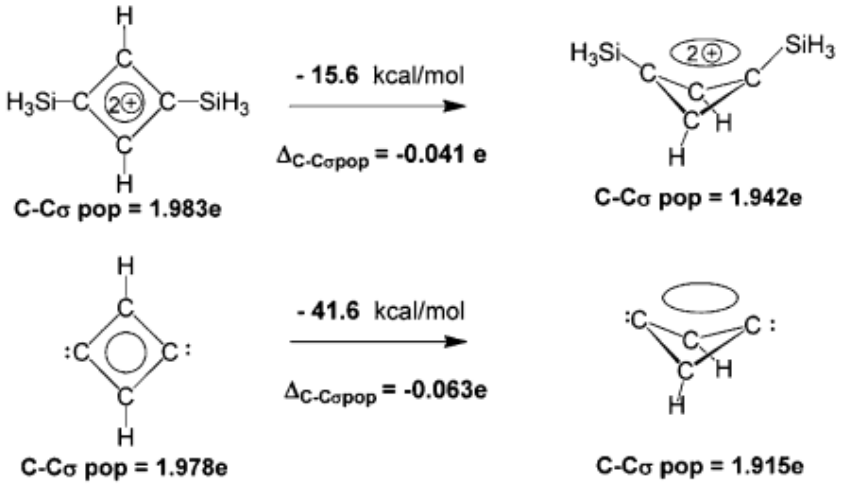

Figure 4-5. B3LYP/6-311+G** inversion barriers and B3LYP/6-31G*//B3LYP/6-311+G** C-C σ NBO occupancies for C_4H_2-$(SiH_3)_2^{2+}$ and C4H2. Electron-donating groups enhance cross ring hyperconjugation, decreasing the occupancy of the strained C-C σ bonds.

Amore subtle approach is required to determine the role of partial 1,3 bonding in stabilizing the puckered conformers of **1a**-**4a**. The NBOs of **1a**, **3a**, and **4a** give no indication of 1,3 bonding, but the CMO to NBO localization of **2a** produces a partially filled 1,3 CC bond orbital corresponding to a combination of folded p_z atomic orbitals, as shown in Figure 3b. The

short 1.802 Å 1,3 C/C distance in **2a** implies a weak bonding interaction not present in the other 2e-aromatic derivatives considered here.

Wiberg Bond Indexes (WBI)[17] are ill-suited for quantifying 1,3 interactions in **1**-**4**. Since puckering enhances the electron density within the rings, 1,3 WBIs increase irrespective of the energetic preferences. Thus, folding increases the 1,3-CC WBIs in both **1a** and **1b** ($C_4F_4^{2+}$) by about 0.038, despite the large destabilization of $C_4F_4^{2+}$ relative to its planar minimum (Figure 4).[18]

Partial 1,3 bonding is not responsible for the puckering of 2π aromatic 4MRs. This is demonstrated definitively by optimizations of partially folded **1a**-**4a** in the absence of cross ring hyperconjugation. While the usual unrestricted optimizations result in the fully puckered conformers of **1a**-**4a**, restricted optimizations, in which the F_{ij} terms corresponding to NBO mixing between the ring σ and p* orbitals are set to zero, lead in each case to the planar conformers (corresponding to the respective planar transition states on the delocalized PES). Thus, even though they are still potentially operative under such constraints, the 1,3-bonding interactions are ineffective. Instead, cross ring hyperconjugation clearly is responsible for the puckering of 4MR-2π e aromatics.

Although 1,3-π overlap is present, in **1a**-**4a** as well as in puckered homoaromatics systems (e.g., the cyclobutenyl cation),[6] it is not the cause of ring puckering in these 4MR systems. These weak 1,3 interactions in 1a-4a have quasi "π" character (see Figure 2, bottom, HOMO b_2 and Figure 3b) and are the residual effects of the 2π electron delocalization stabilization in planar **1a**-**4a** upon puckering. Indeed, both planar and puckered 1a are π-aromatic.[1e,6] Dissected nucleus independent chemical shifts (NICS, at GIAO-PW91/IGLOIII),[19]

$NICS(0)_{\pi zz}$, computed at the heavy atom ring centers of planar (−13.9 ppm) and puckered (−13.4 ppm) 1a are nearly the same (see Figure 6). This is roughly one-third of the $NICS(0)_{\pi zz}$ value for benzene (−35.6 ppm), computed at the same level. For comparison, the $NICS(0)_{\pi zz}$ of the antiaromatic C_4H_4 (D_{2h}) is +58.2 ppm. $NICS_{\pi zz}$ is the most refined NICS index for evaluating π-aromaticity, as it extracts only the out-of-plane (zz) tensor component of the relevant πMOs (or the quasi π HOMO, b_2, for puckered **1a**) involved in aromaticity.

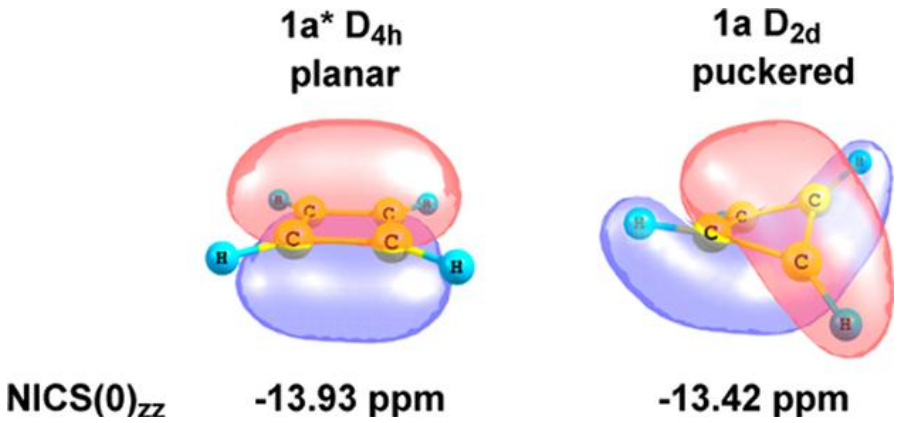

Figure 4-6. Dissected $NICS(0)_{\pi zz}$ values for **1a*** (D_{4h}) and **1a** (D_{2d}) comprising only the $NICS(0)_{zz}$ contributions of the π (and"quasi" π) MOs.

4.4 CONCLUSIONS

Hückel 4MR-2π electron aromatics have only one occupied π MO and no strong preference for planarity. The decrease in vicinal p-π overlap on puckering counteracts any gain in double cross-

ring 1,3 p-overlap. Such p-π effects are not responsible for the puckering of **1a**-**4a**. Instead, the considerable σ-π* mixing (i.e., hyperconjugation across the ring) is responsible for the lower energy of the puckered conformers **1a**-**4a**. Cross-ring hyperconjugation favors non-planar 4MR geometries generally, even for saturated rings (e.g., cyclobutane[20]).

4.5 REFERENCES

(1) (a) Dewar, M. J. S.; McKee, M. L. *Inorg. Chem.* **1978**, *17*, 1569. (b) Krogh-Jespersen, K.; von, P.; Schleyer, R.; Pople, J. A.; Cremer, D. *J. Am. Chem. Soc.* **1978**, *100*, 4301. (c) Bremer, M.; Schleyer, P. v. R.; Fleischer, U. *J. Am. Chem. Soc.* **1989**, *111*, 1147. (d) Radom, L.; Schaefer, H. F. *J. Am. Chem. Soc.* **1977**, *99*, 7552. (e) Balci, M.; McKee, M. L.; Schleyer, P. v. R. *J. Comput. Chem.* **1981**, *2*, 356. (f) Olah, G. A.; Bollinger, J. M.; White, A. M. *J. Am. Chem. Soc.* **1969**, *91*, 3667. (g) Olah, G. A.; Mateescu, G. D. *J. Am. Chem. Soc.* **1970**, *92*, 1432.

(2) (a) Krogh-Jespersen, K.; Cremer, D.; Dill, J. D.; Pople, J.; Schleyer, P. v. R. *J. Am. Chem. Soc.* **1981**, *103*, 2589. (b) Schleyer, P. v. R.; Budzelaar, P. H. M.; Cremer, D.; Kraka, E. *Angew. Chem.* **1984**, *96*, 374. (c) Budzelaar, P. H. M.; Krogh-Jespersen, K.; Clark, T.; Schleyer, P. v. R. *J. Am. Chem. Soc.* **1985**, *107*, 2773. (d) Budzelaar, P. H. M.; Kraka, E.; Cremer, D.; Schleyer, P. v. R. *J. Am. Chem. Soc.* **1986**, *108*, 561. (e) Pilz, M.; Allwohn, J.; B€uhl, M.; Schleyer, P. v. R.; Berndt, A. Z. *Naturforsch.* **1991**, *46b*, 1085. (f) Fokin, A. A.; Kiran, B.; Bremer, M.; Yang, X.; Jiao, H.; Schleyer, P. v. R.; Schreiner, P. R. *Chem. Eur. J.* **2000**, *6*, 1615. (g) Jemmis, E. D.; Subramanian, G.; Korkin, A. A.; Hofmann, M.; Schleyer, P. v. R. *J. Phys. Chem. A* **1997**, *101*, 919. (h) Milburn, R. K.; Bohme, D. K.; Hopkinson, A. C. *Int. J. Mass Spectrom.* **2000**, *195/196*, 393. (i) Sieber, S.; Schleyer, P. v. R.; Otto, A. H.; Gauss, J.; Reichel, F.; Cremer, D. J. *Phys.*

Org. Chem. **1993**, *6*, 445. (j) Chandrasekhar, J.; Schleyer, P. v. R.; Krogh-Jespersen, K. *J. Comput. Chem.* **1981**, *2*, 356.

(3) (a) Hildenbrand, M.; Pritzkow, H.; Zenneck, U.; Siebert, W. *Angew. Chem.* **1984**, *96*, 371. (b) Hornbach, P.; Hildenbrand, M.; Pritzkow, H.; Siebert, W. *Angew. Chem.* **1986**, *98*, 1121. (c) Irngartinger, H.; Hauck, J.; Siebert, W.; Hildenbrand, M. Z. *Naturforsch*. **1991**, *46b*, 1621.

(4) Sahin, Y.; Pr€asang, C.; Amseis, P.; Hofmann, M.; Geiseler, G.; Massa, W.; Berndt, A. *Angew. Chem.* **2003**, *115*, 693.

(5) Mesbah, W.; Pr€asang, C.; Hofmann, M.; Geiseler, G.; Massa, W.; Berndt, A. *Angew. Chem.* **2003**, *115*, 1758.

(6) (a) Olah, G. A.; Staral, J. S.; Spear, R. J.; Liang, G. *J. Am. Chem. Soc.* **1975**, *97*, 5489. (b) Williams, R. V. *Chem. Rev.* **2001**, *101*, 1185. (c) Chen, Z. F.; Jiao, H.; Wu, J. I.; Herges, R.; Zhang, S. B.; Schleyer, P. v. R. *J. Phys. Chem. A* **2008**, *112*, 10586.

(7) Firme, C. L.; Antunes, O. A. C.; Esteves, P. M. *J. Phys. Chem. A* **2007**, *111*, 11094.

(8) Saunders, M.; Laidig, K. E.; Wiberg, K. B.; von, P; Schleyer, R. *J. Am. Chem. Soc.* **1988**, *110*, 7652.

(9) Schoeller, W. W. *J. Am. Chem. Soc.* **1979,** *101*, 4811.

(10) Weinhold, F.; Landis, C. *Valency and Bonding, A Natural Bond Orbital Donor-Acceptor Perspective*; Cambridge University Press: Cambridge, **2005**.

(11) Weinhold, F.; Landis, C. R. *Discovering Chemistry With Natural Bond Orbitals*, **2013**, in preparation.

(12) Hyperconjugation with exocyclic acceptor substituent π*- or p-orbitals decreases the strain of cyclopropane: (a) Hoffmann, R. *Tetrahedron Lett.* **1970**, 2907. (b) Clark, T.; Spitznagel, G.

W.; Klose, R.; Schleyer, P. v. R. *J. Chem. Soc.* **1984**, *106*, 4412. (c) Olah, G. A.; Reddy, V. P.; Prakash, G. K. S. *Chem. Rev.* **1992**, *92*, 69.

(13) Reed, A. E.; Weinstock, R. B.; Weinhold, F. *J. Chem. Phys.* **1985**, *83*, 735.

(14) The sum of the occupancies of the 2s, 2px, and 2p orbitals, comprising the σ-framework of 1b-4b, are decreased relative to 1a-4a, e.g., by −0.716 e for planar 1b vs puckered 1a.

(15) For example, the sum of NPA changes in the 2s, $2p_x$, and $2p_y$ orbitals of each carbon is +0.188 greater in 1c than in 1a.

(16) Hehre, W. J.; Radom, L.; P. v. R. Schleyer, Pople, J. A. *Ab Initio Molecular Orbital Theory*; John Wiley and Sons: **1986**.

(17) Wiberg, K. B. *Tetrahedron* **1968**, *1968*, 1083.

(18) The 1,3 C/C bond indices of planar vs puckered $C_4H_4^{2+}$ are 0.262 and 0.300 respectively, while those of $C_4F_4^{2+}$ are 0.208 and 0.171. F substitution decreases the electron density in the ring center, and smaller absolute bond indices of $C_4F_4^{2+}$ relative to $C_4H_4^{2+}$ result.

(19) (a) Corminboeuf, C.; Heine, T.; Seifert, G.; Schleyer, P. v. R. *Phys. Chem. Chem. Phys.* **2004**, *6*, 273. (b) Fallah-Bagher-Shaidaei, H.; Wannere, C. S.; Corminboeuf, C.; Puchta, R.; Schleyer, P. v. R. *Org. Lett.* **2006**, *8*, 863. (c) Chen, Z.; Wannere, C. S.; Corminboeuf, C.; Puchta, R.; Schleyer, P. v. R. *Chem. Rev.* **2005**, *105*, 3842.

CHAPTER 5

HYPERCOVALENCY AT CARBON? BEYOND THE LEWIS MODEL

- W. C. McKee, K. Ito, I. Fernández, D. Tantillo, P. v. R. Schleyer, To be submitted to *Nat. Chem*.

5.1 ABSTRACT

We report examples of molecules containing a hypervalent carbon bound only to other carbon atoms (C_{hyp}-$(CX)_n$, n = 6, 8), including the first neutral examples of C_{hyp}-$(CX)_n$ octavalency. Unlike many charged hypercoordinate carbon containing species which involve partial ionic bonding between carbon and its ligands, our neutral hexa- and octavalent C_{hyp}-$(CX)_n$ compounds exhibit strictly covalent hypervalency, i.e. *hypercovalency*. The stabilizing hypervalent C-C interactions in these species are due to two-center *electron deficient bonding* (i.e. less than two electrons per bond) which violates the Lewis electron paring rule, but obeys the octet rule. Electron deficient C-C bonds are characterized by a bond critical point, typical C-C bond lengths, and significant energy lowering associated with their formation.

5.2 INTRODUCTION

The bonding capacities of the carbon backbones of approximately 68 million organic compounds are governed by a simple rule: namely that carbon, with its four valence electrons, can form at most four bonds to separate ligands. However an increasing number of molecules containing hypercoordinate carbon atoms are being reported, and it is now clear that such species are not mere theoretical curiosities,[1-9] but rather experimental certainties.[10-18] Still, most currently known examples of hypercoordinate carbons involve metal coordination to the carbon center,[2,3,12,13,15,18] and hence significant ionic character in the C-M bonds. Moreover, the limited number of known (charged) organic hypercoordinate carbon containing compounds,[10,11,14,16,17] most of which achieve hypercoordination by "freezing" SN2 transition state type structures, usually exhibit C-X interactions with heteroatoms of markedly greater electronegativity than carbon, and abnormally long C-X bond lengths.[14,16,17]

These observations, coupled with the remarkable success of elementary Lewis bonding theory,[19] beg a simple question: can carbon achieve hypercoordination through strictly non-polar (i.e. C-C) interactions? If so a distinction should be made between whether the hypercoordinate carbon is merely hypercoordinate, i.e. having more than four nearest neighbors, or also hypervalent. The latter term implies evidence of electron sharing between the hypercoordinate carbon and each of its neighbors and hence the formation of more than four two-center covalent bonds. According to elementary Lewis bonding theory, covalent bonds between atoms are 2-center 2-electron (or multiples thereof in double or triple bonds) interactions between atoms, each of which accommodates no more than 8 electrons (i.e., the "octet rule") in total.[19] Clearly

at least one of these "rules" must be violated in order for carbon to achieve covalent hypervalency, referred to here as *hypercovalency*.

Many examples of molecules containing octet rule violating but Lewis pair preserving hypervalent second row atoms are known. However the bonding in these species is often significantly ionic,[20] precluding hypercovalency. The prospects for finding a comparable hypercovalent carbon compound are even poorer, as carbon has no low lying extra valence orbitals to accommodate more than four 2-electron covalent bonds. However a second mode for achieving carbon hypercovalency has apparently not been considered. We present here evidence of hypercovalency at carbon via an octet rule preserving but Lewis pair violating electron deficient bonding (EDB) mechanism, whereby the hypervalent carbon is covalently bound to more than four carbon atoms via 2-center, less-than-2-electron bonds. This EDB is distinct from the 3-center 2-electron mechanism responsible for bonding in, e.g., the non-classical ethyl cation and CH_5^+.[21]

Before proceeding it is important to ascertain what is meant by a "covalent bond." As no universally accepted quantum mechanical definition of "bonding" currently exists, we shall identify C-C bonds here based on the simultaneous satisfaction of three stringent but intuitive criteria.

1) C-C bond distances must exhibit "normal" lengths.

2) There must be evidence of two-center electron sharing between bound carbons.

3) The formation of C-C bonds must demonstrably lower the energy of the molecule.

The first criteria requires that C-C bond lengths lie between 1.2-1.7 Å; these limits correspond respectively to the common value for C≡C triple bonds, and the longest currently known C-C single bond lengths in alkanes.[22] The second criteria might normally be satisfied by the presence of at least one 2-electron localized molecular orbital (LMO) corresponding to C-C bonding between atomic centers. However the integer occupancy of most LMOs (e.g. Pipek Mezey, Boys, etc.) precludes their use in the identification of 2c-EDBs. We therefore turn directly to the electron density, and identify 2c-electron sharing by the existence of a bond critical point (BCP), i.e., a saddle point in the electron density between two carbon atoms.

As detailed by Bader,[23] the formation of covalent bonds are accompanied by the accumulation of electron charge density between atomic centers. This "crowding" of density between bonded atoms, as shown for ethane in Figure 1, leads to saddle points in the electron density (i.e. BCPS), which are minima along the line of maximum charge density connecting bonded atomic centers, but local maxima along the two axes perpendicular to this (bond) line.

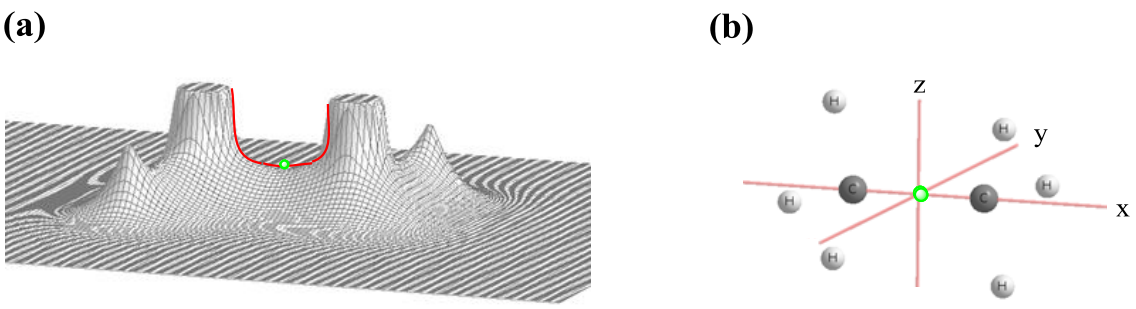

Figure 5-1. **(a)** The electron density of ethane in an H-C-C-H plane, plotted above the plane. The electron density is "crowded" between bonded atomic centers. The C-C BCP (green dot)

and line of maximum charge density connecting the carbons (red line) are also shown above the plane of the nuclei for representational convenience. Spikes in the density correspond to nuclear positions. (b) Depiction of the molecular orientation in (a), and representation of the C-C bond critical point in (a) with origin of the coordinate system taken as the midpoint of the C-C bond (also the C-C BCP location), and the C-C bond as the x axis. The electron density is a local minimum at the BCP along the x axis and a local maximum along the y and z axes. Densities were obtained at the B3LYP/6-311+G** level.

Though BCPs are believed to exist between bound carbons in all classical example of bonding in hydrocarbons,[22] there are a few cases in which BCPs appear between atoms commonly regarded as being in steric contact. For example the "bay hydrogen" in cis-2-butene[23] and planar biphenyl[24] exhibit H-H BCPs, even though the formally non-bonded H/H distances are within the sum of their combined vdW radii (~2.4Å). Moreover the instability of these species relative to their non-H-bonded isomers trans-2-butene and twisted (D_2) biphenyl are generally thought to result from H/H repulsions.[23,24] Hence, as a final criterion for identifying C-C bonds we require that their formation be accompanied by a net lowering of the total molecular energy, as determined by appropriately defined isodesmic or insertion equations.

The stringency of the three criteria for bonding outlined above is illustrated by analysis of the 2-norbornyl cation. Despite its decidedly non-classical geometry,[26] and significant electron delocalization between bridging carbons,[27] its pentacoordinate carbon does not exhibit separate BCPs to its bridging carbon neighbors.[27] Hence there is no 2c charge accumulation between the pentacoordinate carbon the bridging carbons and the 2-norbornyl cation is not hypercovalent by

criteria three. Instead the electron density between the bridging carbons adopts a T-shaped distribution (see Figure 2), consistent with known instances of 3c-2e bonding (e.g., the non-classical ethyl cation and CH_5^+).[23] The markedly different electron density profiles for 3c-2e bonding vs. 2c-EDB are shown in Figure 2.

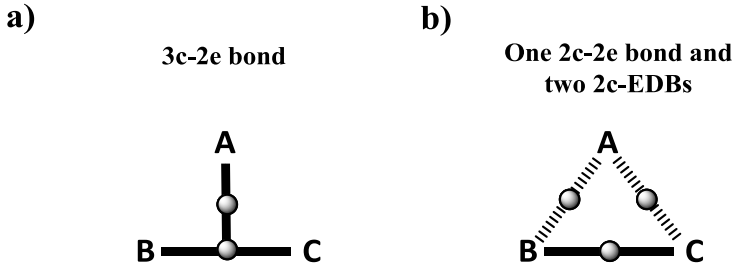

Figure 5-2. a) Electron density profile for a 3-center 2-electon (3c-2e) bond involving hypercoordinate atom A. b) Electron density profile of a hypervalent atom A bound to atoms B and C by electron deficient bonds (EDB). Grey spheres denote bond critical points. Solid and dashed lines denote the lines of maximum charge density connecting atomic centers.

5.3 RESULTS AND DISCUSSION

Before presenting novel species containing hypercovalent carbon atoms, we confirm here that there are at least two experimentally known examples. Masamune's[10] and Hogeveen's[11] cations, which contain penta and hexacoordinate carbon atoms respectively, both exhibit hypercoordinate C-C (C_{hyp}-(CX)) distances in the 1.2-1.7 Å range (with C_{hyp}-(CX) lengths ranging from 1.55-1.64 and 1.71-1.72 Å respectively), and five and six C-C BCPs (respectively) connecting the

hypercoordinate carbons to their neighboring atoms. The stabilization associated with C-C EDB formation in these species is evidenced by the fact that both species are energetically competitive with classically bonded isomers.

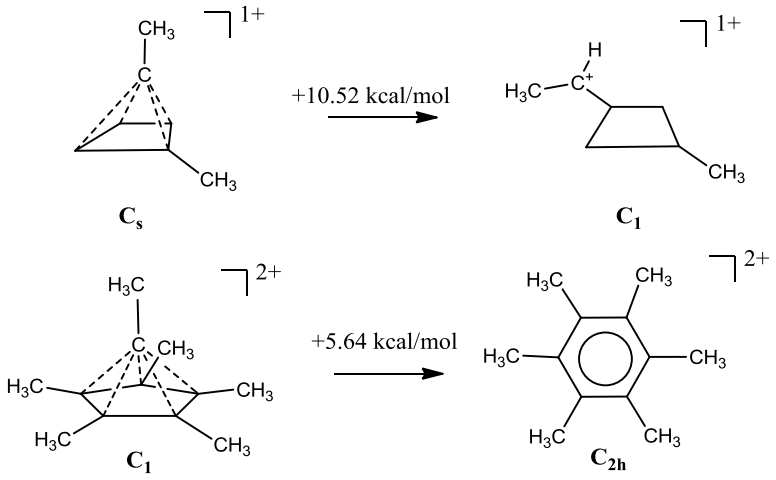

C_s C_1 C_1 C_{2h}

The number of electrons associated with C_{hyp}-(CX) electron deficient bonds can be determined via the electron delocalization index (DI)[28] between C-C centers as defined in the Quantum Theory of Atoms in Molecules (QTAIM).[22] QTAIM DIs measure the number of electron pairs delocalized between two atoms, and serve as a bond order between two carbon atoms connected by a BCP.[29] DI values are well behaved in the sense that the sum of DIs for an octet-rule-preserving carbon atoms is ≈ 4.0, and the DI between the carbon atoms in ethane, benzene, ethylene and acetylene are 1.0, 1.4, 1.9 and 2.9 respectively.[29]

In Masamune's cation, the hypervalent carbon exhibits one 2c-2e bond and four 2c-EDBs. The DI associated with the former bond is 1.01 and the average DI of the four EDBs (which differ individually to the asymmetric position of the hypervalent carbon cap) is 0.75.

Hence the total number of valence electron pairs associated with the hypercovalent carbon is 4.01, and the octet rule is satisfied. A similar situation is observed for Hogeveen's dication where the DI associated with the 2c-2e C-C bond is 1.01, and the average of the DIs associated with the five 2c-EDBs is 0.58, yielding a total electron pair count of 3.91 for the hypercovalent carbon.

We have designed several hydrocarbon dication minima which contain hexacoordinate carbon atoms, **1a**-**4a (**see Figure 3), to test for other examples of hypercovalency. In addition, we also considered examples reported by Minyaev et al. (**5a**),[6] and Wang et al (**6a**).[8]

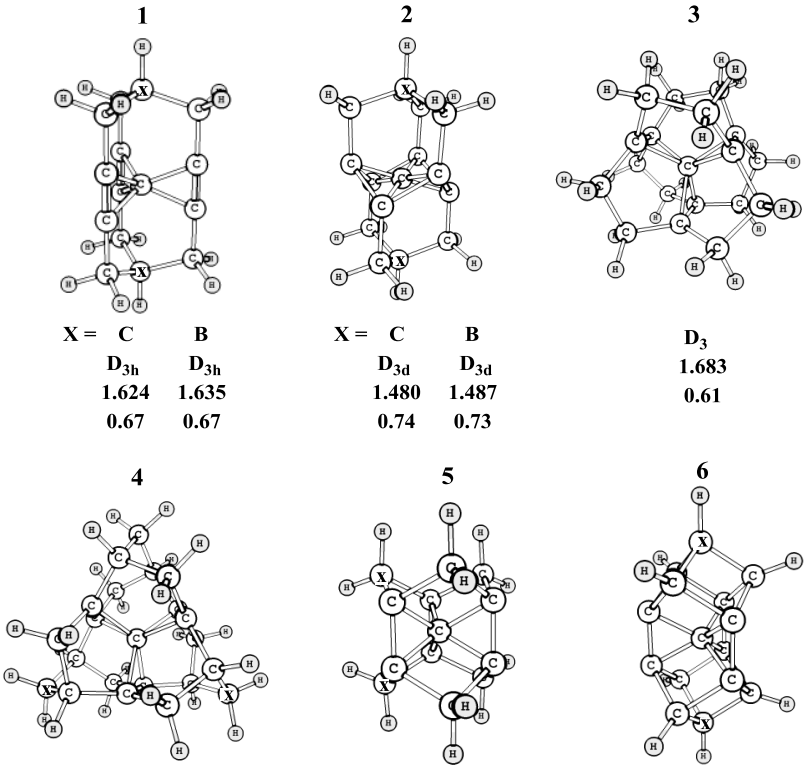

*Avergrage C_{hyp}-C values for non symmetry equivalent electron deficient bonds.

Figure 5-3. Species containing a hexavalent carbon. Replacing atoms marked "X" with carbon atoms gives hydrocarbon dications **1a-6a**. When X=B, neutral hexa-hypercovalent carbon containing structure result (**1b-6b**, except for **3**). Point groups, hypercovalent C-C bond lengths (Å), and hypercovalent C-C DIs are listed in below each molecule. All data are based on B3LYP/6-311+G** computations.

Each of **1a-6a** exhibits C_{hyp}-(CX) distances in the 1.480-1.683 Å range, which are symmetry equivalent within each molecule. Furthermore each hexacoordinate carbon shares a bond critical point with its six neighboring carbon atoms, indicating that it is involved in six distinct C-C bonding interactions. This contrasts with earlier interpretations attributing the C_{hyp}-(CX) interactions in **5a** and **6a** to "multicenter bonding."[6,8] The C_{hyp}-(CX) DIs in **1a-6a** are all close to 2/3. Thus the central carbons in these species follow the octet rule, but violate the Lewis pairing rule by forming of six EDBs instead of four 2c-2e bonds.

We also employed isoelectronic substitution of two carbons in **1a-6a** by two boron atoms to give neutral species **1b-6b** (see Figure 2 with X=B). Except for **3b**, boron substitution resulted in nearly identical structures as for **1a-6a**, with the neutral carborane derivatives retaining their hexacoordinate carbon atoms and the six BCPs to the central carbon. As shown in Figure 2, boron substitution does not significantly affect the C_{hyp}-(CX) bond lengths or DIs. To the best of our knowledge, **1b-2b** and **3b-6b** are the first confirmed examples of neutral hypercovalency,

Wang and coworkers recently reported two tetracation hydrocarbon minima which contain octacoordinate carbons (**7a-8a**, see Figure 4).[8] Based on a similar design strategy, we

located four additional examples of pure hydrocarbon species with an octacoordinate carbon atom (**9a-12a**, Figure 4). **7a-12a** all exhibit bond lengths 1.551-1.567 Å range, close to the prototypical 1.54 Å value associated with normal C-C single bonds.

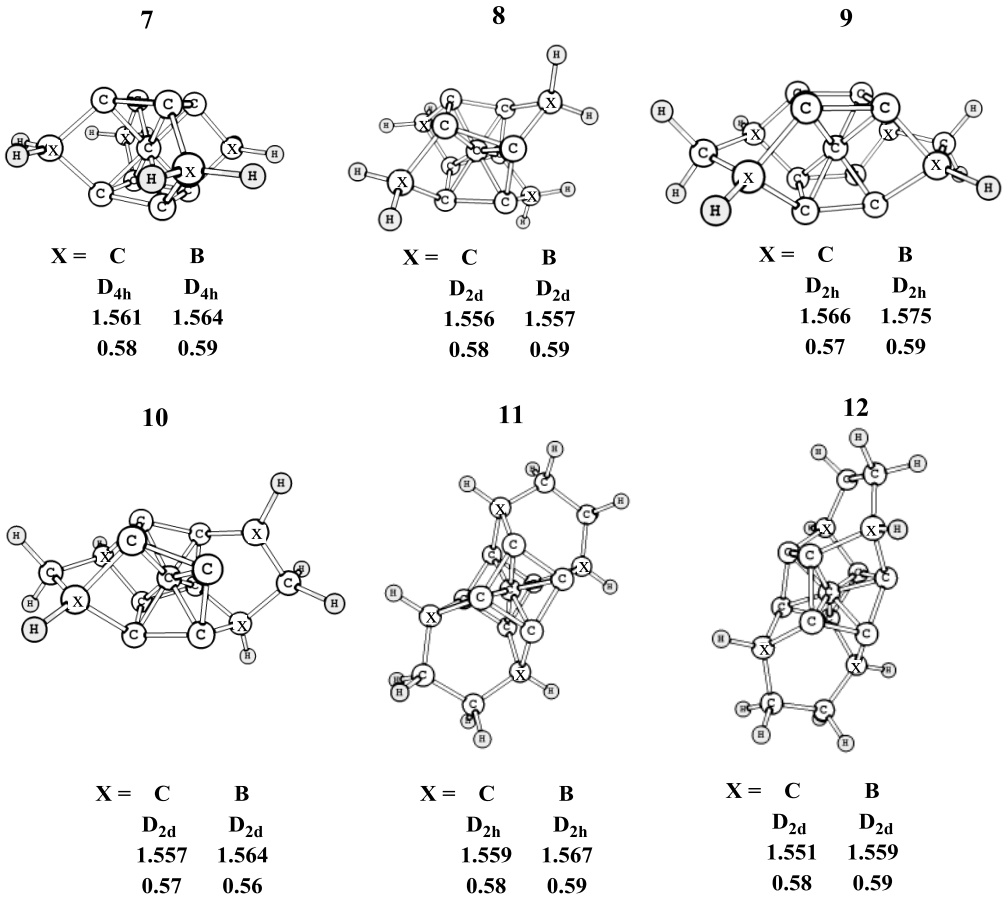

Figure 5-4. Species containing an octavalent carbon. X=C and X=B give tetracation and neutral species **7a-12a**, and **7b-12b** respectively. Point groups, hypercovalent C-C bond lengths (Å), and hypercovalent C-C DIs are listed in below each molecule. All data are based on B3LYP/6-311+G** computations.

Moreover each octacoordinate carbon shares a bond critical point with its eight neighboring carbon atoms, signaling the formation of eight EDBs. Interestingly, the DIs associated with the C_{hyp}-(CX) interactions are all ≈ 0.58, indicating an octet rule violating 4.64 electron pairs associated with the central carbon atoms. This extra density comes from the C_{hyp}-(CX) carbon ligands, which divert a small portion of electron density from their other bonds (as evidence by their DI values being <1), presumably to stabilize the central hypercovalent carbon which formally bears a 4+ charge.

Substituting four carbons in **7a-12a** with boron atoms gives neutral species **7b-12b** (Figure 4). As was the case for the hexa-hypercovalent species in Figure 3, isoelectronic substitution by boron does not appreciably alter the properties of the central hypercoordinate carbon. The C_{hyp}-(CX) distances and DIs are mostly unchanged going from **7a-12a** to **7b-12b**, and the octacoordinate carbon atoms also retain their eight C-C BCPs. **7b-12b** are the first reported examples of both neutral molecules containing an octacoordinate carbon coordinated only to other carbons, and of C_{hyp}-(CX) carbon octa-hypercovalecy.

Each of **1a-12a** may be regarded as an interaction between the unsaturated C-C linkages of a neutral empty cage with a charged carbon atom. In **1a-6a** the hypervalent carbon bears a formal 2+ charge and interacts with three such linkages, and in **7a-12a** the central carbon bears a formal 4+ charge and interacts with four. Thus the energy lowering associated with EDB formation in these species may be evaluated by considering insertion equations of the type:

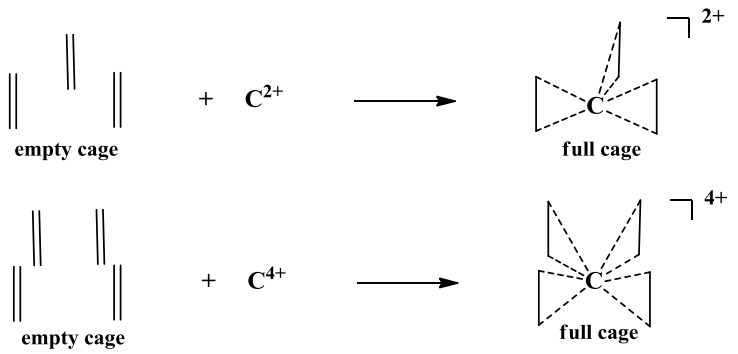

where the empty cage structures are constrained to the geometries they assume in the full cage. Three principle effects contribute to the energy change of these equations. The first is increased steric repulsion accompanying the insertion of a carbon atom into the center of the cage. Second is the purely electrostatic interaction between the positively charged carbon nucleus and the neutral cage. Finally the stabilization afforded by EDB also contributes.

We employed an energy decomposition analysis (EDA)[30,31] to separate the competing contributions to the insertion equations defined above. EDA separates the interaction energy of two fragments (ΔE_{int}) into three components:

$$\Delta E_{int} = \Delta V_{elstat} + \Delta E_{Pauli} + \Delta E_{orb}$$

ΔV_{elstat} corresponds to the classical electrostatic interaction between the two separate fragments obtained by bringing their unmodified charge distributions into the positions they occupy in the complex. ΔE_{Pauli} is the steric repulsion between monomers which results from antisymmetrization and renormalization of the superimposed (overlapping) monomer wavefunctions as required by the Pauli principle. ΔE_{orb} is a stabilizing term arising from orbital

mixing, which is obtained by allowing the orbitals of the complex to relax to their final optimized forms. The adiabatic interaction energy (or bond dissociation energy) between two fragments (D_e) is defined as $-D_e = \Delta E_{prep} + \Delta E_{int}$, where ΔE_{prep} is the energy required to promoted the monomers from their equilibrium structures to the geometries they assume in the complex. We shall focus here mainly on ΔE_{int}.

Compound	***1a***	***2a***	***3a***	***4a***	***5a***	***6a***	***7a***	***8a***	***9a***	***10a***	***11a***	***12a***
ΔE_{int}	-621.8	-532.0	-653.6	-655.5	-530.1	-523.9	-2105.2	-2083.4	-2128.8	-2093.0	-2179.0	-2155.1
ΔE_{Pauli}	816.0	1268.7	795.8	827.4	1056.4	994.4	167.3	172.0	162.3	167.3	167.2	172.1
ΔE_{elstat}[a]	-177.9 (12.4%)	-137.7 (7.6%)	-184.0 (12.7%)	-183.7 (12.4%)	-151.7 (9.6%)	-141.0 (9.3%)	+236.2	+246.1	+235.6	+238.3	+224.7	+230.9
ΔE_{Orb}[a]	-1257.4 (87.4%)	-1660.6 (92.3%)	-1261.3 (87.0%)	-1294.6 (87.3%)	-1432.0 (90.2%)	-1376.1 (90.6%)	-2507.2 (99.9%)	-2500.0 (99.9%)	-2525.2 (99.9%)	-2497.0 (99.9%)	-2568.6 (99.9%)	-2555.7 (99.9%)
ΔE_{disp}[a]	-2.4 (0.2%)	-2.3 (0.1%)	-4.1 (0.3%)	-4.7 (0.3%)	-2.8 (0.2%)	-1.3 (0.1%)	-1.4 (0.1%)	-1.5 (0.1%)	-1.5 (0.1%)	-1.5 (0.1%)	-2.4 (0.1%)	-2.4 (0.1%)
ΔE (=-D_e)	-572.3	-478.8	-609.0	-608.2	-480.2	-475.1	-2043.9	-2015.8	-2067.1	-2029.3	-2112.7	-2089.5
ΔE_{prep}	49.5	53.2	44.6	47.3	49.9	48.8	61.3	67.6	61.7	63.7	66.3	65.6

Table 5-1. Energy decomposition analysis (kcal/mol, BP86-D3/TZ2P) of insertion equations involving **1a-12a**. The values in parentheses give the percentare of the total attractive contribution to ΔE_{int}.

The EDA results are given in Table 1. ΔE_{int} is seen to be significantly stabilizing for all insertion equations involving **1a-12a**; hence there is substantial energy lowering associated with EDB formation and criteria three for hypercovalency is satisfied. Moreover the ΔE_{orb} term, which accounts specifically for covalent orbital mixing and EDB formation, is by far the largest stabilizing contribution to ΔE_{int}. In **1a-6a** stabilization of the carbon atom dication by the electron density of the neutral cage (as evaluated by the V_{elstat} term) accounts for only 10% of the

overall stabilization, while in **7a-12a** the electrostatic interaction between the carbon tetracation and the neutral cages is destabilizing. The magnitude of ΔE_{Pauli} correlates roughly with the C_{hyp}-C bond lengths in **1a-6a**, but is considerably reduced in **7a-12a.** This result is due to the fact that C^{4+} has one less filled valence orbital to overlap with the filled neutral cage orbitals than C^{2+}, and also because this valence orbital is less diffuse (which produces less Pauli exclusion principle violating overlap with the cage orbitals) than those of C^{2+} due to the 4+ vs. 2+ charge on carbon.

Several general characteristics are common to **1a-12a** and **1b-12b**. **1-12** all exhibit unsaturated C-C linkage coordination to the hypercovalent carbon. These units act as 2π-electron donors to the central carbon atom and enable EDB formation. The placement of these linkages within the cage appears to be crucial in determining whether or not the central carbon achieves hypervalency. Cage motifs with C_{hyp}-C distances longer than about 1.70 Å do not exhibit C-C BCPs (the longest C_{hyp}-C distance with a corresponding C-C BCP we observed was 1.702 Å in **4b**). Interestingly this limit corresponds closely to the longest known C-C single bond length value of 1.704 Å.[22]

The roles of the cages themselves are also important in enabling hypercovalency at carbon. The large negative (adiabatic and vertical) energies associated with insertion equations involving **1-12** make it clear that the central carbons are stabilized, rather than "trapped" in an endohedral environment.[32] It is well known that a limiting obstacle to achieving carbon hypercoordination is that the relative shortness of C-X bonds (compared bonds formed by second row atoms) brings its ligands into steric contact.[33] Hence an important functionality of the cages (and saturated C-C linkages) in **1-12** is to minimize ligand-ligand repulsions by ensuring that the closest approaching CX ligands are bonded. This is especially evident in the octavalent carbon

species **7-12**. Other close approaching ligands, which are not bonded, are also fixed into place by the rigid cage structures.

The properties of the electron density topology in **1-12** are also noteworthy. The electron densities at the C_{hyp}-C BCPs range between 0.160-0.226 a.u., or about 70-93% percent of the 0.237 a.u. associated with normal singles bonds. This is mainly attributable to the known relationship between C-C distances and the density at C-C BCPs.[29] More remarkable however is the density at the center of the three membered rings formed by the hypervalent carbon and the unsaturated C-C linkage bridging carbons bond to it. The ring critical point densities, which are points of minimum electron density in the interior of the ring, range from 0.076-0.215 a.u., or about 33-95% of the densities of the BCPs. The similar densities found at the C_{hyp}-C BCPs and RCPs signals major electron delocalization through the ring interiors (this is also evident from the large C_{hyp}-C BCP ellipticitirs), which maximizes C_{hyp}-C bonding by concentrating the density associated with individual EDBs between three centers. Though distinct 2c-EDB formation is clearly apparent from the existence of distnict C_{hyp}-C BCPs, 3c-2e bonds and 2c-EDB evidently exist as two ends of one spectrum as is the case for covalent and ionic bonds.

5.4 CONCLUSIONS

Though it remains to be seen if any of **1-12** can be prepared experimentally, it is likely that many more cages containing hypercovalent carbon atoms can be designed. Moreover as the electron density is a physically observable property, the electron sharing associated with EDB formation (as characterized by the existence of C_{hyp}-C BCPs) is also observable in principle. We note the covalent character of C_{hyp}-C EDBs follow not only from the identical electronegativities of the

hypervalent carbon and its ligand atoms, but also from C_{hyp}-C BCP properties such as the laplacian of the electron density,[23] as well as the energy density[34]. Importantly electron deficient bonding provides an alternative mechanism for carbon to achieve hypervalency, and the extent to which hypercovalency is possible in other atoms presents an intriguing prospect for further study.

5.5 REFERENCES

(1) Jemmis, E. D. Chandrasekhar, J. Würthwein, E-U Schleyer, P. v. R. *J. Am. Chem. Soc.* **1982**, 104, 4275.

(2) Schleyer, P. v. R. Würthwein, E-U. Kaufmann, E. Clark. T. *J. Am. Chem. Soc.* **1983**, 105, 5932.

(3) Schleyer, P. v. R. Kapp, J. *Chem. Phys. Lett.* **1996**, 255, 363.

(4) Wang, Z-X. Schleyer, P. v. R. *Science*. **2001**, 292, 2465.

(5) Wang, Z-X. Schleyer, P. v. R. *Angew. Chem. Int. Ed.* **2002**, 41, 4082.

(6) Minyaev, R. M. Minkin, V. I. Gribanova, T. N. Starikov, A. G. *Mendeleev Comm.* **2004**, 14, 47.

(7) Minyaev, R. M. Gribanova, T. N. Minkin, V. I. *Doklady Chem.* **2004**, 396, 122.

(8) Wang, Y. Huang, Y. Liu, R. *Chem. Eur. J.* **2006**, 12, 3610.

(9) Fernandez, I. Uggerud, E. Frenking, G. *Chem. Eur. J.* **2007**, 13, 8620.

(10) Masamune, S. Sakai, M. Ona, H. Jones, A. J. *J. Am. Chem. Soc.* **1972**, 94, 8956

(11) Hogeveen, H. Kant, P. W. *Acc. Chem. Res.* **1975**, 8, 413.

(12) Kudo, H. *Nature*, **1992**, 355, 432.

(13) Schmidbaur, H. Gabbi, F. P. Schier, A. Riede, J. *Organometallics*, **1995**, 14, 4969.

(14) Akiba, K-y Yamashita, M. Yamamoto, Y. Nagase, S. *J. Am. Chem. Soc.* **1999**, 121, 10644.

(15) Erker, G. *Chem. Soc. Rev.* **1999**, 28, 307.

(16) Yamashita, M. Yamamoto, Y. Akiba, K-y. Hashizume, D. Iwasaki, F. Tagaki, N. Nagase S., *J. Am. Chem. Soc.* **2005**, 127, 4354.

(17) Yamaguchi, T. Yamamoto, Y. Kinoshita, D. Akiba, K-y. Zhang, Y. Reed, C. A. Hashizume, D. Iwasaki, F. *J. Am. Chem. Soc.* **2008**, 130, 6894.

(18) Lancaster, K. M. Roemelt, M. Ettenhuber, P. Hu, Y. Ribbe, M. W. Neese, F. Bergmann, U. DeBeer, S.*Science*, **2011**, 344, 974.

(19) Lewis, G. N. *J. Am. Chem. Soc.* **1916**, 38, 762.

(20) Reed, A. E. Schleyer P. v. R. *J. Am. Chem. Soc.* **1990**, 112, 1434.

(21) Olah, G. A. *Chemical Reactivity and Reaction Paths*; G. Klopman, Ed.; Wilery: London **1974**.

(22) Schreiner, P. R. Chernish, L. V. Gunchenko, P. A. Tikhonchuck, E. Y. Hausmann, H. Serafin, M. Schlecht, S. Dahl, J. E. P. Carlson, R. M. K. Fokin, A. A. *Nature*, **2011**, 477, 308.

(23) Bader, R. F. W. *Atoms in Molecules - A Quantum Theory*; Oxford University Press: New York, **1990**.

(24) Weinhold, F. *J. Comput. Chem.* **2012**, 33, 2440.

(25) Poater, J. Solà, M. Bickelhaupt, F. M. *Chem. Eur. J.* **2006**, 12, 2889.

(26) Scholz, F. Himmel, D. Heinemann, F. W. Schleyer, P. v. R. Meyer, K. Krossing, L. *Science*, **2013**, 341, 62.

(27) Werstiuk, N. H. Muchall, H. M. *J. Phys. Chem. A.* **2000**, 104, 2054.

(28) QTAIM DIs can be derived by integration of the electron pair density over the atomic basins of two atoms. See: Fradera, X. Austen, M. A. Bader, R. F. W. *J. Phys. Chem. A.* **1999**, 103, 304. for full details.

(29) Matta, C. F. Trujillo, J. H. *J. Phys. Chem. A.* **2003**, 107, 7496.

(30) Ziegler, T. Rauk, A. *Theoret. Chem. Acta*. **1977**, 46, 1.

(31) Bickelhaupt, F. M. Baerends, E. J. *Rev. Comput. Chem.* **2000**, 15, 1.

(32) Moran, D. Woodcock, H. L. Chen, Z. Schaefer III, H. F. Schleyer. P. v. R. *J. Am. Chem. Soc.* **2003**, 125, 11442.

(33) Pierrefixe, S. C. A. H. Guerra, C. F. Bickelhaupt, F. M. *Chem. Eur. J.* **2008**, 14, 819.

(34) Cremer, D. Kraka, E. *Croatia Chem. Acta.* **1984**, 57, 1259.

CHAPTER 6

CONCLUSIONS

The current models of bonding and structural stability in hydrocarbons are far from complete. Moving forward we expect that both old (e.g. aromaticity, hyperconjugation) and new (e.g., protobranching, hypercovalency) virtual chemical concepts will continue to aid our understanding of hydrocarbon species, even as these concepts undergo further development and refinement. Several desirable extensions of such concepts are already obvious. For example the generalization of the concept of aromaticity beyond simple non-planar ring systems to fullerenes and other hydrocarbon cages, which are potentially "spherically aromatic," is already underway. Protobranching interactions stabilize alkanes and account for the branching effect, but to what extent do the 1,5 H/H interactions responsible give rise to branching stability in alkenes and alkynes? The energy lowering effects of hyperconjugation are sufficiently large to govern the conformations of small hydrocarbon rings, but its impact on the rotational barriers of simple alkanes, such as ethane, is currently a topic of heated debate. Finally, if carbon can form electron deficient bonds to more than four neighboring carbons in a neutral molecule, what other as yet unknown bonding motifs are possible? These are only a very small sampling of the many unanswered questions related to the properties of hydrocarbons.

Another obstacle to the development of successful models of structure and bonding in hydrocarbons is determining the extent to which the virtual concepts used to explain various behaviors in simple (small) hydrocarbons scale to larger systems relevant to biological and material sciences. Increases in the processing speed and RAM of modern computers have

allowed computational chemists to investigate systems of unprecedented size, and hence unprecedented complexity. How useful are our current models in these environments? For example ring strain and reduced REs resulting from unevenly twisted carbon p AOs limit the energetic stability of small and medium sized Möbius aromatic annulenes. However larger Möbius rings can distribute twisting more evenly, and are also potentially subject to less ring strain. Are any large Möbius 4n π-electron annulenes more stable than their Hückel isomers? Protobranching interactions are the energetically dominant non-covalent interaction in small alkanes, but steric effects (e.g. gauche interactions) become more prevalent as branching increase in larger alkane systems. How does the interplay of attractive and repulsive interactions affect the relative stabilities of large highly branched alkane isomers? Hydrogen bonding is known to significantly impact the secondary and tertiary structures of DNA, but how much of the hydrogen bonding in these species is due to electrostatic effects, and how much is the result of hyperconjugation? The nitrogenase enzyme, which catalyzes the reduction of dinitrogen to ammonia, is believed to contain a hypercoordinate carbon atom. What other molecules relevant to biological and materials science exhibit hypercoordinate carbons?

In closing, we believe that the concepts developed in this thesis contribute to the greater understanding of simple hydrocarbon species. Moreover we hope and expect these finding will be transferrable to larger systems which are being scrutinized increasingly. Hydrocarbon units really are the "backbones" of organic and biological chemistry, and their chemical properties are certain to garner chemist's attention for many years to come.

LIST OF PUBLICATIONS

1. G. E. Douberly, A. M. Ricks, B. W. Ticknor, W. C. McKee, P. v. R. Schleyer, M. A. Duncan, Infrared Photodissociation Spectroscopy of Protonated Acteylene and its Clusters, *J. Phys. Chem. A* **2008**, *112*, 1897.
2. P. v. R. Schleyer, W. C. McKee, Reply to the "Comment on 'The Concept of Protobranching and Its Many Paradigm Shifting Implications for Energy Evaluations' ", *J. Phys. Chem. A* **2010**, *114*, 3737.
3. M. D. Wodrich, W. C. McKee, P. v. R. Schleyer, On the Advantages of Hydrocarbon Radical Stabilization Energies Based on R-H Bond Dissociation Energies *J. Org. Chem.* **2011**, *76*, 2439.
4. W. C. McKee, J. I. Wu, M. Hofmann, A. Berndt, P. v. R. Schleyer, Why do Two π Electron Four-Membered Hückel Rings Pucker?, *Org. Lett.* **2012**, *14*, 5712-5715.
5. W. C. McKee, J. I. Wu, H. S. Rzepa, P. v. R. Schleyer, A Hückel Theory Perspective on Möbius Aromaticity, *Org. Lett.* **2013**, *15*, 3432.
6. W. C. McKee, P. v. R. Schleyer, Correlation Effects on the Relative Stabilities of Alkanes, *J. Am. Chem. Soc.* **2013**, *135*, 13008.
7. W. C. McKee, K. Ito, I. Fernández, D. Tantillo, P. v. R. Schleyer, Hypercovalency at Carbon? Beyond the Lewis Model, **2013**, in preparation for *Nat. Chem.*
8. Y. Mo, C. Wei, J. I. Wu, W. C. McKee, P. v. R. Schleyer, W. Wu, σ-Hyperconjugation in Saturated Hydrocarbon Cages, **2013**, in preparation for *Chem. Eur. J.*